



Review

A review of correlations to model the packing structure and effective thermal conductivity in packed beds of mono-sized spherical particles

W. van Antwerpen^a, C.G. du Toit^{b,*}, P.G. Rousseau^a

^a Post-Graduate School of Nuclear Science and Engineering, North-West University, South Africa

^b School of Mechanical Engineering, North-West University, Hoffman Street, Potchefstroom, North-West Province, 2520 South Africa

ARTICLE INFO

Article history:

Received 28 October 2009

Received in revised form 20 January 2010

Accepted 1 March 2010

ABSTRACT

This paper presents a review of the literature describing the packing structure and effective thermal conductivity of randomly packed beds consisting of mono-sized particles. In this study particular attention was given to the packing structure (porosity, coordination number, and contact angles) and heat transfer by solid conduction, gas conduction, contact area, surface roughness, as well as thermal radiation. New methods to analyse the models were developed giving new insights into the shortcomings of the correlations to predict and define the packing structure, as well as to simulate the effective thermal conductivity in the near-wall region. This information is of particular importance in the design and operation of high temperature packed bed nuclear reactors.

© 2010 Elsevier B.V. All rights reserved.

Contents

1. Introduction.....	1803
2. Packing structure.....	1805
2.1. Porosity.....	1805
2.1.1. Oscillatory porosity correlations (radial direction).....	1805
2.1.2. Oscillatory porosity models (axial direction).....	1806
2.1.3. Exponential porosity correlations (radial direction).....	1806
2.2. Coordination number.....	1807
2.3. Contact angles between adjacent particles.....	1807
2.4. Evaluation of packing structure correlations.....	1807
3. Effective thermal conductivity.....	1809
3.1. Solid and fluid effective thermal conductivity.....	1809
3.2. Effective thermal conductivity with consideration of contact area.....	1810
3.3. Effective thermal conductivity due to thermal radiation.....	1813
3.4. Effective thermal conductivity in the near-wall region.....	1814
3.5. Comparison between effective thermal conductivity correlations.....	1815
4. Conclusion.....	1817
Acknowledgements.....	1817
References.....	1817

1. Introduction

Packed beds are used in various industrial thermal-fluid systems, such as gas-cooled nuclear reactors (Koster et al., 2003), drying processes (Whitaker, 1980), catalytic reactors (Fogler, 1999), processes involving transpiration cooling (Cho and Eckert, 1994),

and high performance cryogenic insulation (Tien and Cunningham, 1973). Since most of these processes are associated with energy transfer, a proper knowledge of the thermal properties of these materials, especially the effective thermal conductivity, is essential to enable the correct design of these thermal systems (Zhou et al., 2007).

A proper understanding of the mechanisms of heat transfer, fluid flow and pressure drop through a packed bed of spheres is of utmost importance in the design of a high temperature pebble bed reactor. Also, a thorough knowledge of the porous structure within the

* Corresponding author. Tel.: +27 18 299 1322; fax: +27 18 299 1320.

E-mail address: Jat.DuToit@nwu.ac.za (C.G. du Toit).

Nomenclature

a	empirical parameter, (Mueller, 1992) absorption coefficient
$a_1 - a_4$	empirical constants (Cohen and Metzner, 1981)
$a_1 - a_4$	empirical constants (Singh and Kaviany, 1994)
a_T	thermal accommodation coefficient
b	empirical parameter (Mueller, 1992)
b	empirical parameter (Suzuki et al., 1981)
b	scattering coefficient
B	empirical deformation parameter
B_r	radiation transmission number, $B_r = f(\varepsilon, \varepsilon_r)$
$B_{r,0}$	Radiation transmission number, $B_{r,0} = f(\varepsilon, 0)$
C_p	specific heat at constant pressure
C	constant parameter in oscillatory porosity correlation, (Martin, 1978)
C	constant parameter in exponential porosity correlations (Vortmeyer and Schuster, 1983; Cheng and Hsu, 1986; Sodré and Parise, 1998; Hunt and Tien, 1990)
D	diameter of cylinder
d_p	diameter of sphere
d	distance of corresponding voids (m)
d	distance between two spheres (m)
d^e	transformed pebble diameter (m)
d_f^e	fluid gap width (m)
d_s^e	solid thickness parameter (m)
E_p	Young modulus (Pa)
F	collinear force (N)
F_E	radiation exchange factor, $F_E = f(\varepsilon, \varepsilon_r)$
F_E^*	radiation exchange factor, $F_E^* = f(A_f, \varepsilon, \varepsilon_r)$
$F_{E,0}$	radiation exchange factor with $F_E = F_E(B = 0)$
h_r	average height of surface roughness (m)
$h(A_f, \varepsilon_r, \varepsilon)$	parameter (Breitbach, 1978)
H	height of a packed bed (m)
J_0	Bessel function of the first kind
j	j th sphere
k_{bed}	total effective thermal conductivity ($\text{W m}^{-1} \text{K}^{-1}$)
k_{eff}	effective thermal conductivity due to thermal conduction and radiation ($\text{W m}^{-1} \text{K}^{-1}$)
$k_{f,eff}$	effective thermal conduction due to fluid mixing (braiding effect) ($\text{W m}^{-1} \text{K}^{-1}$)
k_{rs}	thermal conductivity due to radiation from a solid to a solid
k_{rv}	Thermal conductivity due to radiation from a void to a void
$k_{s,eff}$	effective thermal conductivity due to solid particle movement ($\text{W m}^{-1} \text{K}^{-1}$)
k_f	thermal conductivity of fluid or gas phase
k_G	thermal conductivity with variance in gas pressure ($\text{W m}^{-1} \text{K}^{-1}$)
k_e^r	effective thermal conductivity due to radiation ($\text{W m}^{-1} \text{K}^{-1}$)
k_e^c	effective thermal conductivity through contact area ($\text{W m}^{-1} \text{K}^{-1}$)
k_e^g	effective thermal conductivity through fluid/gas and point contact ($\text{W m}^{-1} \text{K}^{-1}$)
$k_e^{g,c}$	Combination of effective thermal conductivities k_e^g and k_e^c ($\text{W m}^{-1} \text{K}^{-1}$)
k_s	thermal conductivity of solid phase ($\text{W m}^{-1} \text{K}^{-1}$)
Kn	$\equiv \lambda/d$ Knudsen number
K	combination parameter
l_v, l_s	effective lengths
l	modified mean free path of gas molecules (m)

M_g	molecular mass of gas (kg kmol^{-1})
M_s	molecular mass of solid surface (kg kmol^{-1})
M^*	effective molecular mass (kg kmol^{-1})
N	parameter in exponential porosity correlations
N	parameter (Bauer and Schlünder, 1978)
\bar{N}_c	average coordination number
N_A	number of particles per unit area
N_L	number of particles per unit length
n	coordination flux number
P	gas pressure (Pa)
p	external contact pressure acting on spheres (Pa)
Q	heat flux (W)
R	outer radius of cylindrical packed bed (m)
R	radiation reflection number
\tilde{R}	universal gas constant
R_i	inner radius of annulus (m)
R_o	outer radius of annulus (m)
r	radial coordinate
r_p	radius of sphere (m)
r_c	radius of the contact area (m)
$r_{0,j}$	distance from adjacent sphere to origin of sphere under consideration (m)
r_1	radius to considered sphere centre point (m)
S	packing variable
S_F	packing variable
s	contact area parameter
T	temperature (K)
T_s	solid surface temperature (K)
T_0	$\equiv 273 \text{ K}$
\bar{T}	average temperature (K)
ΔT	Temperature difference (K)
W	$\equiv (R_o - R_i)$ width of annular packed bed (m)
x	dimensionless distance
x	coordinated in the x direction
z	particle diameters from a wall
z_m	particle diameter parameter

Greek symbols

α_0	deformation factor
α	$\equiv 90^\circ - \phi_c$ ($^\circ$)
β	empirical parameter
γ	constant parameter
γ_a	effective length ratio
γ_c	effective length ratio
δ	contact area between two spheres (m^2)
ε	porosity or void fraction
ε_{\min}	minimum porosity in near-wall region
ε_b	bulk porosity
ε_0	reference porosity
$\bar{\varepsilon}$	average porosity
ε_∞	Porosity of infinite bed
ε_r	emissivity
ε'_r	Effective emissivity
ε_{wall}	constant porosity in the near-wall region
θ_c	contact angle [radians]
θ_0	angle corresponding to boundary of heat flow area for one contact point [radians]
κ	dimensionless parameter $\equiv k_s/k_f$
κ_r	radiation ratio parameter
κ_G	gas conduction ratio in Knudsen regime parameter
λ	mean free path of gas molecules (m)
μ	$\equiv M_g/M_s$ molecular mass ratio between gas and solid surface

μ_p	Poisson ratio
π	pi
σ	Stephan–Boltzmann constant $\sigma = 5.67 \times 10^{-8}$ (W m ⁻² K ⁻⁴)
τ	radiation reflection and transmission parameter ratio
$\bar{\phi}_c$	average contact angle in the radial position (°)
ϕ_c	critical zenithal angle (°)
φ	contact area fraction parameter
χ	radiation exchange ratio
ψ	radiation reflection and transmission parameter ratio
ψ_t	heat transfer parameter
ψ_1	heat transfer parameter calculated by ψ_{1or2} with $n = 1.5$
ψ_2	heat transfer parameter calculated by ψ_{1or2} with $n = 4\sqrt{3}$
ψ_{1or2}	heat transfer parameter
Δ_0	dimensionless weighting function
Δ_f	dimensionless solid conductivity
BCC	basic centred cubic packing
CT	computed tomography
CAT	computed axial tomography
DEM	discreet element method
FCC	face-centred cubic packing
HTTU	high temperature test unit
MRI	magnetic resonance imaging
PFC3D	particle flow code 3D
SC	simple cubic packing
ZBS	Zehner, Bauer, and Schlünder model

packed bed is important to any rigorous analysis of the transport phenomena, since the heat and flow mechanisms are influenced by the porous structure (Van Antwerpen et al., 2009). Usually, the heat exchange takes place through an adjacent wall. The heat transfer inside the solid/fluid–gas system, as well as between the solid/fluid–gas system and this adjacent wall, are phenomena consisting of different components dependant on various operating conditions (Bauer, 1990).

The effective thermal conductivity in high temperature packed bed reactors is usually derived by lumping all the relevant heat transfer mechanisms into a single representative value. This value is used to simulate heat transfer under normal operating and severe upset conditions. According to Bauer (1990) the concept of the effective thermal conductivity of a packed bed (k_{bed}) can be split into three contributing components.

The first component is that of the effective thermal conductivity (k_{eff}) of a packed bed saturated with a stagnant fluid consisting of four distinct heat transfer mechanisms, namely: (1) conduction through the solid; (2) conduction through the contact area between adjacent particles accounting for surface roughness; (3) conduction through the stagnant fluid/gas phase; and (4) radiation between solid surfaces.

The second component is that of the enhanced fluid effective thermal conductivity ($k_{f,eff}$) due to the turbulent mixing of the fluid flowing through the interstices of the packing in parallel with the wall while the solid phase is motionless, also referred to as the braiding effect (Bauer and Schlünder, 1978). This turbulent mixing can be described as moving turbulent fluid pockets, criss-crossing between the particles and exchanging energy. This has the effect of increasing the total effective thermal conductivity through the packed bed.

The third component is present where the fluid phase as well as the solid phase is in motion ($k_{s,eff}$). Introducing, an additional enhancement of heat transfer occurring in the solid phase due to the motion of the particles. The effective thermal conductivity k_{bed} of the bed is therefore given by:

$$k_{bed} = k_{eff} + k_{f,eff} + k_{s,eff} \quad (1)$$

The focus of this study is to review the different published methodologies to simulate the porous structure and the total effective thermal conductivity (k_{eff}).

2. Packing structure

The thermal design of a packed bed such as a pebble bed reactor (PBR) is based upon the mechanisms of heat and mass transfer, and the flow and pressure drop of the fluid through the bed of solids (Kugeler and Schulten, 1989; Nuclear Safety Standards Commission (KTA), 1981). The mechanisms in turn are all sensitive to the porous structure of the packed bed (White and Tien, 1987).

Most of the difficulties encountered in predicting the effective thermal conductivity are associated with the fact that the effective thermal conductivity is a phenomenological characterization of a solid–fluid medium rather than a thermo-physical property (Aichlmayr and Kulacki, 2006). Therefore, before any heat transfer analysis is attempted, one should have a thorough understanding of the structural arrangement of the packed bed under consideration.

In a PBR the porous structure varies sharply near a wall, since there the geometry of the packing is altered. This wall effect occurs in two situations, namely the effect of the side walls (radial direction) and the effect of the top- and bottom walls (axial direction). The latter is referred to by Zou and Yu (1995) as the thickness effect that is obviously dependant on the height of the packed bed. The wall effect, both in the radial and axial directions, is defined in this study to occur over a distance of five particle diameters $0 \leq z \leq 5$ from the wall. Both of these effects will be investigated due to the importance they have on all the associated phenomena. The investigation will comprise of experimental and numerical results, where the numerical results were generated using the discrete element method (DEM) code PFC3D, (Anon, 1999).

2.1. Porosity

The correlations most often employed to characterize the friction factor (Nuclear Safety Standards Commission (KTA), 1981), the Nusselt numbers for heat transfer between the walls and the gas and the pebbles and the gas (Kugeler and Schulten, 1989), as well as the effective thermal conductivity (Zehner and Schlünder, 1972) are commonly based, amongst others, on the porosity. In this study the presence of the particles is modelled implicitly using a pseudo-heterogeneous approach.

Du Toit (2008) stated that the correlations to predict the variation in porosity can be classified into two categories, i.e. those that attempt to describe the oscillatory behaviour of the variation in the porosity and those that attempt to describe the variation of the averaged porosity using an exponential expression. Both of these methods will be investigated. It should be noted that the porosity is considered to be uniform in the tangential direction, i.e. an axially symmetric approach.

2.1.1. Oscillatory porosity correlations (radial direction)

Table 1 gives a summary of the relevant correlations to determine the oscillatory variation in the porosity in the radial direction of cylindrical, as well as annular packed beds. Some cylindrical correlations were rewritten to account for annular configurations. It is important to note that in Table 1 and Table 2, R_i refers to the

Table 1
Summary of the correlations for the oscillatory variation in porosity in the radial direction.

Reference	
Martin (1978)	<p>Correlation (Cylindrical)</p> $\varepsilon(x) = \begin{cases} \varepsilon_{\min} + (1 + \varepsilon_{\min})x^2, & -1 \leq x < 0 \\ \varepsilon_b + (\varepsilon_{\min} - \varepsilon_b)e^{-x/4} \cos\left(\frac{\pi}{C}x\right), & x \geq 0 \end{cases} \quad (2)$ <p>Parameters</p> $x = 2 \frac{R-r}{d_p} - 1 \quad (3)$ $C = \begin{cases} 0.816 & D/d_p = \infty \\ 0.876 & D/d_p = 20.3 \end{cases} \quad (4)$ $\varepsilon_{\min} = 0.20 - 0.26 \quad (5)$
Cohen and Metzner (1981)	<p>Correlation (Cylindrical)</p> $\frac{1 - \varepsilon(z)}{1 - \varepsilon_b} = 4.5 \left[z - \frac{7}{9}z^2 \right] \quad z \leq 0.25 \quad (6)$ $\frac{\varepsilon(z) - 1}{1 - \varepsilon_b} = a_1 e^{(-a_2 z)} \cos[a_3 z - a_4] \pi \quad 0.25 < z < 8 \quad (7)$ $\varepsilon(z) = \varepsilon_b \quad 8 \leq z \leq \infty \quad (8)$ <p>Parameters</p> $z = \frac{R-r}{d_p} \quad a_1 = 0.3463, a_3 = 2.4509 \quad a_2 = 0.4273, a_4 = 2.2011 \quad (9)$
Ridgway and Tarbuck (1968) and Kamiuto et al. (1989)	<p>Correlation (Annular)</p> <p>For $0 \leq z \leq 0.6$</p> $\varepsilon(z) = 1 - 3.10036z + 3.70243z^2 - 1.24612z^3 \quad (10)$ <p>For $0.6 < z \leq (R_0 - R_i)/2d_p$</p> $\varepsilon(z) = -0.1865 \exp\left(-0.22z_m^{1.5}\right) \cos(7.66z_m) + \varepsilon_b \quad (11)$ <p>Parameters</p> $z = \frac{r - R_i}{d_p}, \quad R_i \leq r \leq \frac{R_0 + R_i}{2} \quad (12)$ $z = \frac{R_0 - r}{d_p}, \quad \frac{R_0 + R_i}{2} \leq r \leq R_0 \quad (13)$ $z_m = z - 0.6 \quad (14)$
Mueller (1992)	<p>Correlation (Cylindrical)</p> $\varepsilon(r) = \varepsilon_b + (1 - \varepsilon_b) J_0\left(a \frac{r}{d_p}\right) \times \exp\left(-b \frac{r}{d_p}\right) \quad (15)$ <p>Parameters</p> $a = \begin{cases} 7.45 - \frac{3.15}{D/d_p} & 2.02 \leq D/d_p \leq 13.0 \\ 7.45 - \frac{11.25}{D/d_p} & 13.0 < D/d_p \end{cases} \quad (16)$ $b = 0.315 - \frac{0.725}{D/d_p}, \quad \varepsilon_b = 0.365 + \frac{0.22}{D/d_p} \quad (17)$
De Klerk (2003)	<p>Correlation (Annular)</p> $\varepsilon(z) = 2.14z^2 - 2.53z + 1 \quad z \leq 0.637 \quad (18)$ $\varepsilon(z) = \varepsilon_b + 0.29 \exp(-0.6z) \times [\cos(2.3\pi(z - 0.16))] + 0.15 \exp(-0.9) \quad z > 0.637 \quad (19)$ <p>Parameters</p> $z = \frac{r - R_i}{d_p}, \quad R_i \leq r \leq \frac{R_0 + R_i}{2} \quad (20)$ $z = \frac{R_0 - r}{d_p}, \quad \frac{R_0 + R_i}{2} \leq r \leq R_0 \quad (21)$

inner radius of the annulus and R_0 to the outer radius of an annular packed bed, while R refers to the outer radius of a cylindrical bed.

Many versions of the correlation proposed by Mueller (1991) exist (Mueller, 1992, 1999, 2002, 2005). However, Theuerkauf et al. (2006) showed that the Bessel function does not give an accurate representation of the void fraction in the near-wall region between $0 \leq z \leq 0.5$. For this reason the correlation developed by Mueller (1992) is only quoted for the sake of completeness.

2.1.2. Oscillatory porosity models (axial direction)

Zou and Yu (1995) remarked that most investigations into the variation of the porosity was done for the radial direction and only considered the side wall effect, whilst implicitly assuming that the thickness effect is negligible. Zou and Yu (1995) also stated that the error due to this assumption is usually so small that it can be ignored for most cases. However, it must be considered for some situations where the height of the packed bed is small. Zou and Yu (1995) studied the dependence of the bulk porosity on d_p/H under loose and dense randomly packed conditions by considering a cylindrical packed bed with $d_p/D = 3/74$. The results showed that the bulk porosity of both the dense and loose randomly packed beds start to

increase when $d_p/H > 0.05$. A variation in the bulk porosity between $0.395 < \varepsilon_b \leq 0.46$ was observed in the dense randomly packed case when $0.05 < d/H \leq 0.4$. No correlations were proposed.

2.1.3. Exponential porosity correlations (radial direction)

In some models, it is assumed that the “averaged” porosity decays exponentially from the wall (Vortmeyer and Schuster, 1983). Table 2 gives a summary of all relevant correlations based on this assumption.

The parameter ε_0 was taken by Vortmeyer and Schuster (1983), Cheng and Hsu (1986) and Hunt and Tien (1990) to be equal to the bulk porosity, $\varepsilon_0 = \varepsilon_b$, whilst Sodr  and Parise (1998) took $\varepsilon_0 = \varepsilon_\infty$, where ε_∞ is defined as the porosity of an infinite bed (Sodr  and Parise, 1998). As Du Toit (2008) explained, the value of C is taken to give a porosity of 1 at the wall interface. Therefore, Cheng and Hsu (1986) assumed $C = 1$, where the value of N was taken to be $N = 2$ by Vortmeyer and Schuster (1983) and Cheng and Hsu (1986), whilst Hunt and Tien (1990) used a value of $N = 6$ for spherical particles. Furthermore, Sodr  and Parise (1998) proposed that the value of N be obtained from Eq. (24), which must be solved iteratively and the average bed porosity for the annulus is given by Eq. (25).

Table 2

Summary of the correlations for the exponential variation in the averaged porosity in the radial direction.

Reference	Correlation (Annular)	
Vortmeyer and Schuster (1983)	$\varepsilon(r) = \varepsilon_0 \left[1 + C \exp \left(-N \frac{r - R_i}{d_p} \right) \right]$	$R_i \leq r \leq \frac{R_0 + R_i}{2}$ (22)
Cheng and Hsu (1986)		
Sodré and Parise (1998)	$\varepsilon(r) = \varepsilon_0 \left[1 + C \exp \left(-N \frac{R_0 - r}{d_p} \right) \right]$	$\frac{R_0 + R_i}{2} \leq r \leq R_0$ (23)
Hunt and Tien (1990)		
Sodré and Parise (1998)	Parameters	
	$N = \frac{2C\varepsilon_\infty d_p [1 - \exp(-N(R_0 - R_i)/2d_p)]}{(\bar{\varepsilon} - \varepsilon_\infty)(R_0 - R_i)}$	(24)
	$\bar{\varepsilon} = 0.3517 + 0.387 \frac{d_p}{2(R_0 - R_i)}$	(25)
	Correlation (Annular)	
White and Tien (1987)	$\varepsilon(r) = \left[1 + \left(\frac{1 - \varepsilon_b}{\varepsilon_b} \right) \sqrt{1 - \exp \left(-2 \frac{r - R_i}{d_p} \right)} \right]^{-1}$	for $R_i \leq r \leq \frac{R_0 + R_i}{2}$ (26)
	$\varepsilon(r) = \left[1 + \left(\frac{1 - \varepsilon_b}{\varepsilon_b} \right) \sqrt{1 - \exp \left(-2 \frac{R_0 - r}{d_p} \right)} \right]^{-1}$	for $\frac{R_0 + R_i}{2} \leq r \leq R_0$ (27)

2.2. Coordination number

The coordination number, defined as the number of particles in contact with the particle under consideration is very useful to model transport phenomena through packed beds (Goodling and Khader, 1985). A summary of the correlations proposed by various authors to predict the average coordination number as a function of the bulk porosity of a packed bed is given in Table 3 (Du Toit et al., 2009).¹

Du Toit et al. (2009) noted that significant differences can be observed when these correlations are compared with one another (see Fig. 4) and emphasized that the empirical correlations shown in Table 3 are not valid in the near-wall region, although some boundary conditions clearly state the validity up to a porosity of one. Most of the empirical correlations draw an analogy between the coordination numbers of ordered packings and the coordination number of a randomly packed bed with the same porosity as mentioned in Van Antwerpen et al. (2009). Therefore, Du Toit et al. (2009) showed that the coordination number in the near-wall region differs significantly from that previously predicted in the bulk region by the correlations.

2.3. Contact angles between adjacent particles

Du Toit et al. (2009) defined a contact angle between two adjacent particles as the angle between the line connecting the centre points of two particles in contact with each other and the line perpendicular to the direction of the heat flux. Although using contact angles is a relatively new approach in characterizing packing structures, authors such as Sui and Lee (2000) recognized the potential of contact angles in simulating the effective thermal conductivity. A contact angle of $\phi_c = 0^\circ$ implies that the heat transfer between the two particles in contact does not contribute to the heat flux in the relevant coordinate direction, whilst a contact angle of $\phi_c = 90^\circ$ implies maximum contribution to the heat flux (see Fig. 1). Du Toit et al. (2009) also analyzed the variation of the average contact angle $\bar{\phi}_c$ in the radial direction of a numerically packed bed and obtained the following relation between \bar{N}_c and $\bar{\phi}_c$:

$$\bar{\phi}_c = -6.1248\bar{N}_c^2 + 73.419\bar{N}_c - 186.68 \quad (40)$$

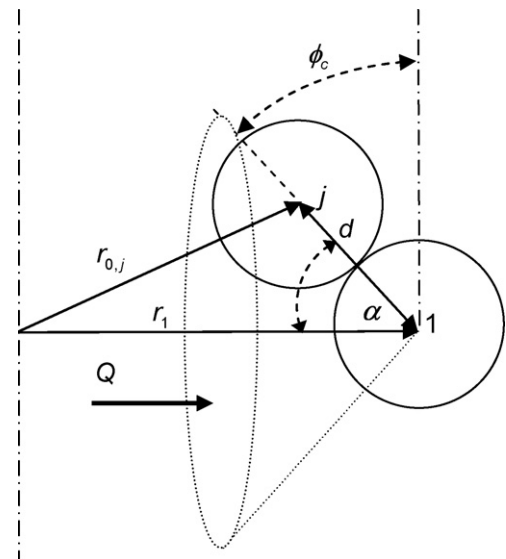
where the coordination number \bar{N}_c can be obtained from Eq. (39).

2.4. Evaluation of packing structure correlations

Various authors performed experiments to obtain the variation in the voidage of packed beds in the bulk and near-wall regions (Roblee et al., 1958; Benenati and Brosilow, 1962; Scott, 1962; Thadani and Peebles, 1966; Ridgway and Tarbuck, 1966, 1968; Staněk and Eckert, 1979; Goodling et al., 1983; Küfner and Hofmann, 1990; Mueller, 1992; Giese et al., 1998).

Although many different experimental techniques were used, the results are in general agreement. A good overview of the experimental methods used by the various authors is given in De Klerk (2003). However, for the purpose of this study, porosity results obtained from the analysis of numerically generated annular packed beds and physical experimental data obtained by Du Toit (2008) is used to evaluate the different porosity correlations displayed in Tables 1 and 2.

Two sets of experiments were performed by Du Toit (2008), representing two scale models of an annular geometry. A similar approach to that of Goodling et al. (1983) was followed to manufacture the packed beds and obtain the results. The spheres consisted of 3.6 mm lead balls and the interstices were filled with epoxy

**Fig. 1.** Contact angle between two spheres (Du Toit et al., 2009).

¹ Note the + in the last term of Eq. (12) in Du Toit et al. (2009) should be –.

Table 3

Summary of the empirical correlations for the average coordination number as function of the bulk porosity.

Reference	Correlation (for bulk region)	Validity
Rumpf (1958)	$\bar{N}_c = 3.1/\varepsilon$	$(0.2595 \leq \varepsilon \leq 1)$ (28)
Meissner et al. (1964)	$\bar{N}_c = 2e^{2.4(1-\varepsilon)}$	$(0.2595 \leq \varepsilon \leq 1)$ (29)
Ridgway and Tarbuck (1968)	$\varepsilon = 1.072 - 0.1193\bar{N}_c + 0.00431\bar{N}_c^2$	$(0.2595 \leq \varepsilon \leq 1)$ (30)
Haughey and Beveridge (1969)	$\bar{N}_c = 22.47 - 39.39\varepsilon$	$(0.2595 \leq \varepsilon \leq 0.5)$ (31)
Nakagaki and Sunada (1968)	$\bar{N}_c = 1.61\varepsilon^{-1.48}\bar{N}_c = 4.28 \times 10^{-3}\varepsilon^{-17.3} + 2$	$(\varepsilon \leq 0.82)$ (32)
Smith et al. (1929)	$\bar{N}_c = 26.49 - 10.73/(1 - \varepsilon)$	$(\varepsilon > 0.82)$ (33)
Gotoh (1978)	$\bar{N}_c = 20.7(1 - \varepsilon) - 4.35$	$(\varepsilon \leq 0.595)$ (34)
		$(0.3 \leq \varepsilon \leq 0.53)$
		$(\varepsilon > 0.53)$
Suzuki et al. (1981)	$\bar{N}_c = 36(1 - \varepsilon)/\pi$ $\bar{N}_c = 2.812 \frac{(1-\varepsilon)^{-1/3}}{(b/d_p)^2 [1 + (b/d_p)^2]}$ where $(1 - \varepsilon)^{-1/3} = \frac{1 + (b/d_p)^2}{1 + (b/d_p)e^{(b/d_p)^2} \text{Erfc}(d_p/b)}$	$(0.2595 \leq \varepsilon \leq 1)$ (35)
Yang et al. (2000)	$\bar{N}_c = 2.02 \frac{1+87.38(1-\varepsilon)^4}{1+25.81(1-\varepsilon)^4}$	$(0.39 \leq \varepsilon \leq 1)$ (37)
Zhang et al. (2001)	$\bar{N}_c = \frac{1}{0.183-659.248(1-\varepsilon)^{20.967}}$	$(0.37 \leq \varepsilon \leq 0.45)$ (38)
Reference	Correlation (for bulk and near-wall region)	Validity
Du Toit et al. (2009)	$\bar{N}_c = 25.952\varepsilon^3 - 62.364\varepsilon^2 + 39.724\varepsilon - 2.0233$	$(0.2398 \leq \varepsilon \leq 0.54)$ (39)

resin. In all cases the particle diameter to annular width ratio was $d_p/W = 14.12$.

Du Toit (2008) noted that the two sets of experimental results exhibited the same damped oscillatory behaviour in the variation of the porosity in the radial direction ranging from a maximum at the walls to the bulk value in the centre part of the annulus.

Thereafter, Du Toit (2008) developed a numerical procedure to extract the radial and axial porosities from numerically generated packed beds. Good agreement was obtained between the experimental and numerical results obtained with PFC3D.

For the correlations evaluated in Fig. 2, the bulk porosity was taken as $\varepsilon_b = 0.385$ which is the value obtained in the numerical results. In the case of the correlation proposed by Martin (1978), the minimum porosity was taken as $\varepsilon_{\min} = 0.245$ in accordance with the numerical results and the constant in the equation as $C = 0.876$.

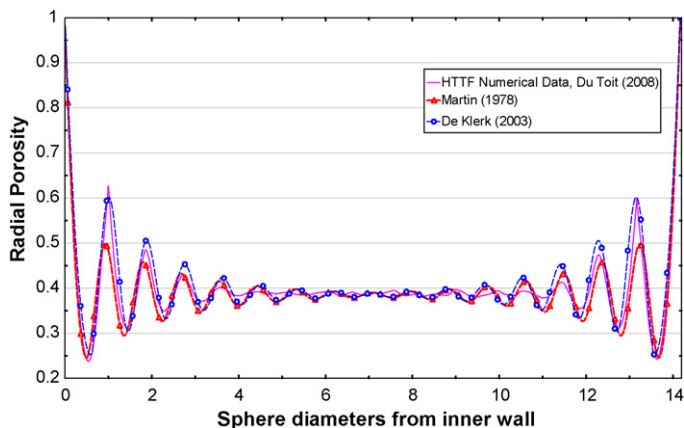
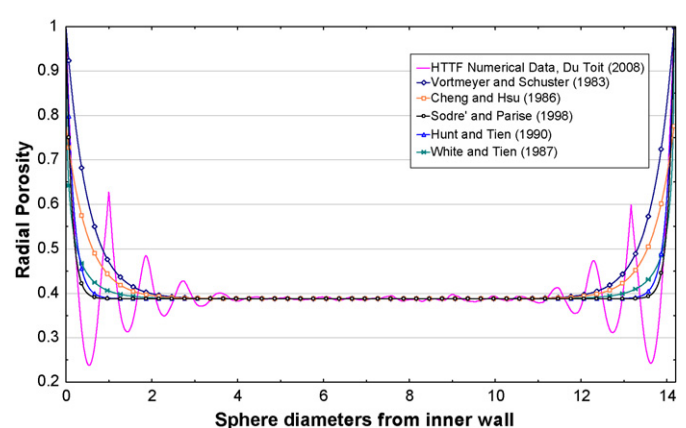
Du Toit (2008) emphasized that in the case of the Cohen and Metzner (1981) correlation the dimensionless distance x from both walls in the middle of the annulus is less than 8 and the correlation therefore never achieves the bulk value for the porosity.

Also as mentioned previously, Theuerkauf et al. (2006) stated that due to the nature of the Bessel function employed by Mueller (1992) the predicted variation in the porosity next to the wall leads to an over-prediction of porosity. Thus, the correlation of Mueller (1992) is not taken into account in this evaluation.

Du Toit (2008), found that the correlation proposed by Martin (1978) to be the most representative of numerical results. However, after comparing the correlations displayed in Table 1 with the numerical results of Du Toit (2008), it was found that the correlation proposed by De Klerk (2003) gives an even better prediction of the variation in the radial porosity than Martin (1978) (see Fig. 2).

The comparison between the exponential porosity correlations displayed in Table 2 and numerical results for the heat transfer test facility (HTTF) is shown in Fig. 3. Du Toit (2008) noted that the correlation derived by Sodré and Parise (1998) failed to relate with the results obtained by the other correlations and proposed that ε_∞ be substituted by ε_b in the bulk region of the annulus and $\bar{\varepsilon}$ with the average porosity for the annulus obtained from the numerical results. After a careful examination by Du Toit (2008) it was found that the correlation proposed by Hunt and Tien (1990) gives the best representation of the “averaged” variation of porosity in the radial direction.

The number of experimental studies conducted to determine the average coordination number in the bulk and near-wall region is far less than the number of experimental studies performed to determine the variation of porosity in the radial direction. Much controversy exists about the experimental data giving the relationship between the coordination number and radial porosity in packed beds. The controversy is due to the fact that various researchers (Roblee et al., 1958; Scott, 1962; Benenati

**Fig. 2.** Comparison between radial oscillatory porosity correlations.**Fig. 3.** Comparison between radial exponential porosity correlations.

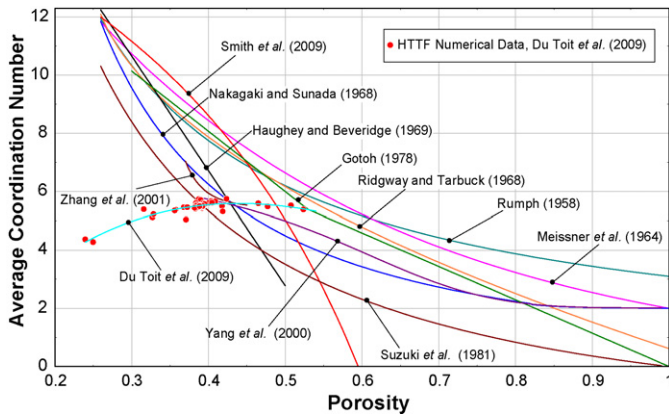


Fig. 4. Comparison between different coordination number correlations.

and Brosilow, 1962; Thadani and Peebles, 1966; Ridgway and Tarbuck, 1966; Staněk and Eckert, 1979; Suzuki et al., 1981; Goodling et al., 1983; Goodling, 1985; Küfner and Hofmann, 1990; Kaviani, 1991; Giese et al., 1998; Yang et al., 2000; Sui and Lee, 2000; Zhang et al., 2001) based their models on taking an analogy between ordered packings with a certain porosity and randomly packed beds with the same porosity as mentioned previously.

Goodling (1985) did an experimental study to obtain the average radial coordination number for spheres with $d_p = 6.35$ mm in a cylindrical packed bed. A reduction in the coordination number nearing the near-wall region was noted with an average coordination number of 8 in the bulk region. The same reduction in the coordination number in the near-wall region was noted in the numerical results by Du Toit et al. (2009) with $d_p = 60$ mm. Du Toit et al. (2009) found an average coordination number in the bulk region of 5.52. Sederman et al. (2001) followed a different methodology and determined the most probable coordination number to occur using magnetic resonance imaging (MRI). They investigated various D/d_p ratio's in cylindrical packed beds with sphere diameters ranging from $d_p = 2$ –5 mm. The results showed that the most probable coordination number to occur ranged between 5 and 6. Another method used to determine the coordination number in a packed bed is to employ a computed tomography (CT) or CAT scanner. Georgalli and Reuter (2006) successfully used a CT scanner to determine the coordination number in a multi-sized randomly packed bed. Their results showed that the coordination number of multi-sized sphere beds with particle diameters ranging for various experiments between $d_p = 4.5$ –9.5 mm, varied from 6.27 to 7.57.

Because of this controversy in the experimental data to determine the coordination number, Du Toit et al. (2009) decided to use numerical data to analyze the radial coordination number in a randomly packed bed. Fig. 4 shows the comparison between the predictions by the correlations of the average coordination number as a function of porosity.

The correlation proposed by Suzuki et al. (1981) gives an accurate prediction of the average coordination number in the bulk region where the porosity is in the order of $\varepsilon \approx 0.39$ (see Fig. 4). However, the correlation fails to predict the coordination number elsewhere. This can be attributed to the critical zenithal angle φ_c in their numerical model (defined by Suzuki et al., 1981) that does not provide an accurate representation of the variation of the coordination number as a function of porosity.

Lastly, Du Toit et al. (2009) found the average contact angle in the bulk region of the numerically generated randomly packed bed that they analyzed to be $\varphi_c = 31.97^\circ$.

3. Effective thermal conductivity

In this study the effective thermal conductivity k_{eff} is divided into three components (heat transfer mechanisms), the effective conductivity k_e^g through the fluid and point contact, the effective conductivity k_e^c through contact area and the effective conductivity k_e^r due to radiation. The following summations give total effective thermal conductivity k_{eff} :

$$k_{eff} = k_e^g + k_e^c + k_e^r \quad (41)$$

or

$$k_{eff} = k_e^{g,c} + k_e^r \quad (42)$$

where $k_e^{g,c}$ is the combination of k_e^g and k_e^c .

3.1. Solid and fluid effective thermal conductivity

In this section all the correlations defining the effective thermal conductivity through the solid and fluid phases with stagnant flow and point contact conduction will be discussed. These models neglect thermal radiation.

Deissler and Boegli (1958) noted that the maximum effective thermal conductivity for a two-phase system is given by a unidirectional heat flow through parallel layers of solid and fluid phases (Eq. (43)) and the minimum by a series arrangement (Eq. (44)).

$$\frac{k_e^{g,c}}{k_f} = \varepsilon + (1 - \varepsilon)\kappa \quad (43)$$

$$\frac{k_e^{g,c}}{k_f} = \frac{1}{\varepsilon + (1 - \varepsilon)/\kappa} \quad (44)$$

where $\kappa = k_s/k_f$. These two correlations also act as the bounds for the other effective thermal conductivity correlations.

Kunii and Smith (1960) developed a correlation for a porous structure by discretizing the solid and fluid phase into separate modes acting in series and parallel. They defined the effective lengths l_v and l_s which correspond to the lengths of the parallel and series regions. Ultimately the effective thermal conductivity correlation is given by:

$$\frac{k_e^g}{k_f} = \varepsilon + \frac{\beta(1 - \varepsilon)}{\psi_t + \gamma/\kappa} \quad (45)$$

where the empirical value $\beta = 0.895$ for a close packing of spheres and $\beta = 1$ for a loosely packed bed. The empirical value of γ depends on l_s and was found to be $\gamma = 2/3$. The empirical constant ψ_t is a function of the number of contacts responsible for heat transfer, defined by Du Toit et al. (2009) as the coordination flux number n . For the basic loose packing Kunii and Smith (1960) argued that $n = 1.5$ and for a close packing $n = 4\sqrt{3}$. ψ_t is then approximated by:

$$\psi_t = \psi_2 + (\psi_1 + \psi_2) \frac{\varepsilon - 0.260}{0.216} \quad \text{for } 0.260 \leq \varepsilon \leq 0.476 \quad (46)$$

where ψ_1 correspond to $\psi_{1 \text{ or } 2}$ evaluated for the loose and packing arrangements and ψ_2 evaluated for the close packing arrangement.

$$\psi_{1 \text{ or } 2} = \frac{0.5(\kappa - 1/\kappa)^2 \sin^2 \theta_0}{\ln(\kappa - (\kappa - 1)\cos \theta_0) - (\kappa - 1/\kappa)(1 - \cos \theta_0)} - \frac{2}{3\kappa} \quad (47)$$

where θ_0 [radians] is the fraction of the total heat transfer associated with one contact point between two spheres. This angle can be calculated by:

$$\sin^2 \theta_0 = 1/n \quad (48)$$

Zehner and Schlünder (1970) considered the effective thermal conductivity through a cylindrical unit cell containing both the solid

and fluid phases. The critical part of the correlation is that [Zehner and Schlünder \(1970\)](#) have drawn an analogy between mass transfer experiments done by [Currie \(1960\)](#) and thermal conduction to obtain an empirical curve to describe the effective thermal conductivity for $0 \leq \varepsilon \leq 1$. Important to note is that this curve was obtained from mass transfer experiments done in the bulk region of packed beds with specific porosities. An analogy between a bulk porosity of a specific value and a near-wall porosity with the same value cannot be made as previously mentioned. For that reason one can conclude that the [Zehner and Schlünder \(1970\)](#) correlation is not valid in the near-wall region. This ties in with the observation made by [Thurgood et al. \(2004\)](#) who demonstrated the shortcomings of the [Bauer and Schlünder \(1978\)](#) model in the near-wall region. The [Bauer and Schlünder \(1978\)](#) model is a refinement of the [Zehner and Schlünder \(1970\)](#) correlation which is discussed later on in the study.

Nonetheless, the effective thermal conductivity correlation of [Zehner and Schlünder \(1970\)](#) based on a unit cell is given by:

$$\frac{k_e^g}{k_f} = [1 - \sqrt{1 - \varepsilon}] + \frac{2\sqrt{1 - \varepsilon}}{1 - \kappa^{-1}B} \cdot \left[\frac{(1 - \kappa^{-1})B}{(1 - \kappa^{-1}B)^2} \ln\left(\frac{1}{\kappa^{-1}B}\right) - \frac{B+1}{2} - \frac{B-1}{1 - \kappa^{-1}B} \right] \quad (49)$$

The deformation parameter B is related to the porosity by $B = 1.25((1 - \varepsilon)/\varepsilon)^{10/9}$. However, [Hsu et al. \(1994\)](#) found that $B = 1.364(1 - \varepsilon)/\varepsilon^{1.055}$ results in a more accurate prediction.

[Okazaki et al. \(1977\)](#) derived a model using the same methodology applied by [Kunii and Smith \(1960\)](#). One distinct difference is that the coordination heat flux number is $n = \tilde{N}_c/6$ and that the average coordination number is related to porosity by Eq. (30). Investigating the correlation proposed by [Okazaki et al. \(1977\)](#) it was found to give inappropriate values compared to the other correlations and therefore neglected in this study.

[Batchelor and O'Brien \(1977\)](#) derived a correlation with the focus on particle-to-particle contact. They assumed an analogy between electrical and thermal conductivity. This assumption can be questioned because [Tsotsas and Martin \(1987\)](#) stated that certain features of heat transfer in packed beds with a fluid phase cannot be simulated with equivalent electric systems. This holds for the thermal radiation as well as for the pressure dependence of the thermal conductivity of the fluid in confined spaces. Nonetheless, after fitting an empirical curve through the experimental data the following correlation was obtained:

$$\frac{k_e^g}{k_f} = 4.0 \ln\left(\frac{k_s}{k_f}\right) - 11 \quad (50)$$

Note that Eq. (50) is not an explicit function of porosity due to the assumed packing arrangement in the bulk region.

[Cheng et al. \(1999\)](#) presented an alternative approach to determine the effective thermal conductivity of a packed bed consisting of mono-sized spheres, in the presence of a stagnant fluid. They considered the packing structure in a microscopic manner using Voronoi polyhedra ([Hindrichsen and Wolf, 2006](#)). However, to implement this model, the coordinates of the packing structure must be obtained to be able to calculate some of the Voronoi polyhedron parameters. Their model is, therefore, mentioned in this study for the sake of completeness.

[Sui and Lee \(2000\)](#) developed a method to calculate the effective thermal conductivity for the solid phase of a packed bed considering structured packings. This method is only valid for packed beds with porosities below 0.5 and where the conductivity of the solid phase is much larger than that of the surrounding fluid matrix. This is equivalent to calculating the effective thermal conductivity of a packed

bed under vacuum conditions. They considered a randomly packed bed, to be based on three different ordered structures, depending on porosity, i.e. a simple cubic (SC), body-centre cubic (BCC) or face-centre cubic (FCC) packing. [Sui and Lee \(2000\)](#) further developed a resistance correlation for each contact angle (SC = 90°, BCC = 35.27°, and FCC = 45°). However, this correlation will not be discussed further due to the fact that the model is only valid for the solid phase of a packed bed.

3.2. Effective thermal conductivity with consideration of contact area

Various authors, e.g. ([Zhou et al., 2007](#); [Hsu et al., 1994](#); [Hsu et al., 1995](#); [Aichlmayr and Kulacki, 2006](#)), described the importance of contact area at high solid to fluid thermal conductivity ratios, $\kappa \geq 10^3$. The occurrence of these finite contact areas is attributed by [Hsu et al. \(1994\)](#) to external loads acting onto the spherical particles or due to their own weight acting upon a contact in a packed bed.

One fundamental difference that must be pointed out is that of contact area and particle surface roughness. Contact area is defined as the contact region between two particles, which increase in size with external load due to the elasticity of the solid material. Whereas, surface roughness being a characteristic of the two areas in contact which determines the effective thermal contact area. This leads to the presence of the Smoluchowski effect as described in [Kennard \(1938\)](#) where a reduction in conduction occurs through the small gas-filled gaps in the contact area.

The thermal conductivity of dilute gases is, according to the molecular theory of gases, independent of pressure. This is valid only as long as the mean free path λ of the gas molecules is small compared to the geometrical dimension d of the corresponding voids ([Tsotsas and Martin, 1987](#)). The thermal conductivity of a gas changes when the Knudsen number ($Kn = \lambda/d$) enters the transition region $Kn \leq 10$ as described by [Bahrami et al. \(2004a\)](#). Smoluchowski discovered the same effect earlier in 1898. Thus, the reduction of the thermal conductivity in gasses when $Kn \leq 10$ will hereafter be referred to as the Smoluchowski effect. An in-depth explanation of this phenomenon can be obtained in [Springer \(1971\)](#). This section, therefore, illustrates some models considering heat transfer through contact area, particle roughness or a combination thereof.

Inspired by the one-dimensional lumped parameter model of [Kunii and Smith \(1960\)](#), [Hsu et al. \(1995\)](#) developed three lumped parameter models to calculate the effective thermal conductivity in porous media. [Hsu et al. \(1995\)](#) firstly considered a two-dimensional unit cell model comprised of contacting square cylinders, the so-called square cylinder model. This model is based on a simplified discontinuous fluid phase model of [Nozad et al. \(1985a\)](#). The correlation for the effective thermal conductivity proposed by [Hsu et al. \(1995\)](#) is given by:

$$\frac{k_e^{g,c}}{k_f} = \gamma_a \gamma_c \kappa + \frac{\gamma_a(1 - \gamma_c)}{1 + (\kappa^{-1} - 1)\gamma_a} + \frac{(1 - \gamma_a)}{1 + (\kappa^{-1} - 1)\gamma_a \gamma_c} \quad (51)$$

where the geometric parameter γ_a is related to porosity and the adjustable parameter γ_c through:

$$1 - \varepsilon = \gamma_a^2 + 2\gamma_c \gamma_a(1 - \gamma_a) \quad (52)$$

and where γ_c is the same parameter used by [Nozad et al. \(1985a\)](#) in their numerical calculations. [Hsu et al. \(1995\)](#) found that $\gamma_c = 0.01$ yields the best agreement with the experimental data obtained by [Nozad et al. \(1985b\)](#).

[Hsu's et al. \(1995\)](#) second correlation was developed by replacing the connecting square cylinders with an array of adjoining circular cylinders. The geometric parameter γ_a is related to porosity

and the adjustable parameter γ_c for this correlation through:

$$\varepsilon = 1 - \gamma_c \gamma_a - \left(\frac{\gamma_a^2}{2} \right) \left(\frac{\pi}{2} - 2\theta_c \right) \quad (53)$$

where the contact angle is defined as $\theta_c = \sin^{-1}(\gamma_c)$. The effective thermal conductivity can be calculated by three expressions each for a specific range of κ as displayed in Eqs. (54)–(56).

Hsu et al. (1995) found that when using the cylinder model $\gamma_c = 0.01$ gave the best agreement with the experimental data. Aichlmayr and Kulacki (2006) stated that the cylinder model gives unrealistic estimates for the effective thermal conductivity when $\kappa < 100$. However, in the current study it was found that the model does give realistic values (see Fig. 6). Presumably, this indicates that Aichlmayr and Kulacki (2006) might have made an error in their implementation of the correlation.

(i) For $(1/\kappa - 1)\gamma_a < 1$

$$\begin{aligned} \frac{k_e^{g,c}}{k_f} = & \gamma_c \gamma_a \kappa + \frac{1 - \gamma_a \sqrt{1 - \gamma_c^2}}{\gamma_a \gamma_c \left(\frac{1}{\kappa} - 1 \right) + 1} + \frac{\kappa \left(\frac{\pi}{2} - 2\theta_c \right)}{1 - \kappa} \\ & - \frac{2\kappa}{(1 - \kappa) \sqrt{1 - \left(\frac{1}{\kappa} - 1 \right)^2 \gamma_a^2}} \\ & \times \left[\tan^{-1} \left[\frac{\tan \left(\frac{\pi}{4} - \frac{\theta_c}{2} \right) + \left(\frac{1}{\kappa} - 1 \right) \gamma_a}{\sqrt{1 - \left(\frac{1}{\kappa} - 1 \right)^2 \gamma_a^2}} \right] \right. \\ & \left. - \tan^{-1} \left[\frac{\tan \left(\frac{\theta_c}{2} \right) + \left(\frac{1}{\kappa} - 1 \right) \gamma_a}{\sqrt{1 - \left(\frac{1}{\kappa} - 1 \right)^2 \gamma_a^2}} \right] \right] \end{aligned} \quad (54)$$

(ii) For $(1/\kappa - 1)\gamma_a > 1$

$$\begin{aligned} \frac{k_e^{g,c}}{k_f} = & \gamma_c \gamma_a \kappa + \frac{1 - \gamma_a \sqrt{1 - \gamma_c^2}}{\gamma_a \gamma_c \left(\frac{1}{\kappa} - 1 \right) + 1} + \frac{\kappa \left(\frac{\pi}{2} - 2\theta_c \right)}{1 - \kappa} \\ & - \frac{\kappa}{(1 - \kappa) \sqrt{\left(\frac{1}{\kappa} - 1 \right)^2 \gamma_a^2 - 1}} \\ & \times \left[\ln \left[\frac{\tan \left(\frac{\pi}{4} - \frac{\theta_c}{2} \right) + \left(\frac{1}{\kappa} - 1 \right) \gamma_a - \sqrt{\left(\frac{1}{\kappa} - 1 \right)^2 \gamma_a^2 - 1}}{\tan \left(\frac{\pi}{4} - \frac{\theta_c}{2} \right) + \left(\frac{1}{\kappa} - 1 \right) \gamma_a + \sqrt{\left(\frac{1}{\kappa} - 1 \right)^2 \gamma_a^2 - 1}} \right] \right. \\ & \left. - \ln \left[\frac{\tan \left(\frac{\theta_c}{2} \right) + \left(\frac{1}{\kappa} - 1 \right) \gamma_a - \sqrt{\left(\frac{1}{\kappa} - 1 \right)^2 \gamma_a^2 - 1}}{\tan \left(\frac{\theta_c}{2} \right) + \left(\frac{1}{\kappa} - 1 \right) \gamma_a + \sqrt{\left(\frac{1}{\kappa} - 1 \right)^2 \gamma_a^2 - 1}} \right] \right] \end{aligned} \quad (55)$$

(iii) For $(1/\kappa - 1)\gamma_a = 1$

$$\begin{aligned} \frac{k_e^{g,c}}{k_f} = & \frac{\gamma_c \gamma_a^2}{\gamma_a + 1} + \frac{1 - \gamma_a \sqrt{1 - \gamma_c^2}}{\gamma_c + 1} + \gamma_a \left(\frac{\pi}{2} - 2\theta_c \right) \\ & - \left[\tan \left(\frac{\pi}{4} - \frac{\theta_c}{2} \right) - \tan \left(\frac{\theta_c}{2} \right) \right] \end{aligned} \quad (56)$$

Hsu et al. (1995) extended the touching square cylinder model by considering a three-dimensional unit cell consisting of cubes. The following relation was obtained:

$$\begin{aligned} \frac{k_e^{g,c}}{k_f} = & 1 - \gamma_a^2 - 2\gamma_c \gamma_a + 2\gamma_c \gamma_a^2 + \gamma_c^2 \gamma_a^2 \kappa + \frac{\gamma_a^2 - \gamma_c^2 \gamma_a^2}{\left[1 - \gamma_a + \gamma_a \left(\frac{1}{\kappa} \right) \right]} \\ & + \frac{2 \left(\gamma_c \gamma_a - \gamma_c \gamma_a^2 \right)}{\left[1 - \gamma_c \gamma_a + \gamma_c \gamma_a \left(\frac{1}{\kappa} \right) \right]} \end{aligned} \quad (57)$$

The geometric parameters γ_a and γ_c are related to porosity by:

$$1 - \varepsilon = \left(1 - 3\gamma_c^2 \right) \gamma_a^3 + 3\gamma_c^2 \gamma_a^2 \quad (58)$$

Hsu et al. (1995) found that for the cube model $\gamma_c = 0.13$ resulted in the best agreement with the experimental data.

Bauer and Schlünder (1978) improved the model developed by Zehner and Schlünder (1970) by including thermal radiation, considering the Knudsen regime (Smoluchowski effect) and introducing a surface fraction parameter φ for heat transfer through contact areas. This improved correlation is commonly known as the Zehner, Bauer, and Schlünder (ZBS) model. The effective thermal conductivity k_{eff} can be calculated as follows:

$$\begin{aligned} \frac{k_{eff}}{k_f} = & (1 - \sqrt{1 - \varepsilon}) \varepsilon \left[\left(\varepsilon - 1 + \frac{1}{\kappa_G} \right)^{-1} + \kappa_r \right] \\ & + \sqrt{1 - \varepsilon} [\varphi \kappa + (1 - \varphi) \kappa_c] \end{aligned} \quad (59)$$

where

$$\begin{aligned} \kappa_c = & \frac{2}{N} \left\{ \frac{B(\kappa + \kappa_r - 1)}{N^2 \kappa_G \kappa} \ln \frac{\kappa + \kappa_r}{B[\kappa_G + (1 - \kappa_G)(\kappa + \kappa_r)]} \right. \\ & \left. + \frac{B + 1}{2B} \left[\frac{\kappa_r}{\kappa_G} - B \left(1 + \frac{1 - \kappa_G}{\kappa_G} \kappa_r \right) \right] - \frac{B - 1}{N \kappa_G} \right\} \end{aligned} \quad (60)$$

and

$$N = \frac{1}{\kappa_G} \left(1 + \frac{\kappa_r - B \kappa_G}{\kappa} \right) - B \left(\frac{1}{\kappa_G} - 1 \right) \left(1 + \frac{\kappa_r}{\kappa} \right) \quad (61)$$

Again B is the deformation parameter presented by Zehner and Schlünder (1970). The radiation parameter is given by:

$$\kappa_r = \frac{k_e^r}{k_f} = \frac{4\sigma}{\left(\frac{2}{\varepsilon_r} - 1 \right)} T^3 \frac{d_p}{k_f} \quad (62)$$

whilst the gaseous conduction is related to the Knudsen regime by:

$$\kappa_G = \frac{k_G}{k_f} = \left[1 + \left(\frac{l}{d_p} \right) \right]^{-1} \quad (63)$$

where l is a modified free path of gas molecules defined by:

$$l = 2 \frac{2 - a_T}{a_T} \left(\frac{2\pi \tilde{R} T}{M_g} \right)^{1/2} \cdot \frac{k_f}{P(2C_p - \tilde{R}/M_g)} \quad (64)$$

with T the absolute temperature in [K], P gas pressure [Pa], \tilde{R} the universal gas constant, M_g the molecular mass of the gas, k_f the molecular thermal conductivity of the gas outside the Knudsen regime, k_G the thermal conductivity as function of gas pressure, k_e^r the thermal radiative conductivity and a_T the thermal accommodation coefficient. The thermal accommodation coefficient a_T as defined by Bahrami et al. (2006a) represents the degree to which the kinetic energy of a gas molecule is exchanged when it collides with a solid surface. Song and Yovanovich (1987) proposed a correlation to estimate a_T for engineering surfaces, given by:

$$\begin{aligned} a_T = & \exp \left[-0.57 \left(\frac{T_s - T_0}{T_0} \right) \right] \left(\frac{M^*}{6.8 + M^*} \right) \\ & + \frac{2.4\mu}{(1 + \mu)^2} \left\{ 1 - \exp \left[-0.57 \left(\frac{T_s - T_0}{T_0} \right) \right] \right\} \end{aligned} \quad (65)$$

where

$$M^* = \begin{cases} M_g & \text{for monoatomic gases} \\ 1.4M_g & \text{for diatomic/polyatomic gases} \end{cases}$$

with $T_0 = 273K$, T_s the solid surface temperature and $\mu = M_g/M_s$ the ratio between the molecular masses of the gas and the solid surface.

It must be emphasized that [Bauer and Schlünder \(1978\)](#) noted that the contact area fraction ϕ is a function of many undetermined limiting quantities such as the elasticity of the material, external mechanical stress, and condition of the surface of the material. They also mentioned that the contact area must be obtained experimentally. However, a first order estimate is obtained for the surface fraction parameter ϕ in Section 3.5 by comparing the correlation with experimental data.

[Hsu et al. \(1994\)](#) questioned the validity of the model proposed by [Zehner and Schlünder \(1970\)](#) at solid to fluid thermal conductivity ratios above $\kappa \geq 10^3$. They postulated that the reason why the [Zehner and Schlünder \(1970\)](#) model under-predicts the stagnant thermal conductivity of a packed bed consisting of spherical particles under these conditions is that the model assumes point contacts between spheres rather than finite contact areas. Therefore, [Hsu et al. \(1994\)](#) argued that the [Zehner and Schlünder \(1970\)](#) model could be improved by incorporating the effects of particle-to-particle contacts through a finite contact area. The resulting effective thermal conductivity of the unit cell is then given by:

$$\begin{aligned} \frac{k_e^{g,c}}{k_f} = & \left[1 - \sqrt{(1-\varepsilon)} \right] + \frac{\sqrt{(1-\varepsilon)}}{\kappa^{-1}} \left(1 - \frac{1}{(1+\alpha_0 B)^2} \right) \\ & + \frac{2\sqrt{(1-\varepsilon)}}{[1-\kappa^{-1}B + (1-\kappa^{-1})\alpha_0 B]} \left(\frac{(1-\kappa^{-1})(1+\alpha_0)B}{[1-\kappa^{-1}B + (1-\kappa^{-1})\alpha_0 B]^2} \right. \\ & \times \ln \left(\frac{1+\alpha_0 B}{(1+\alpha_0)B\kappa^{-1}} \right) - \frac{B+1+2\alpha_0 B}{2(1+\alpha_0 B)^2} \\ & \left. - \frac{(B-1)}{[1-\kappa^{-1}B + (1-\kappa^{-1})\alpha_0 B](1+\alpha_0 B)} \right) \end{aligned} \quad (66)$$

The introduction of the contact parameter causes the geometric deformation parameter B , in Eq. (66) to become a function of α_0 . Consequently, B is determined iteratively from:

$$\begin{aligned} \varepsilon = 1 - & \frac{B^2}{(1-B)^6(1+\alpha_0 B)^2} \times \left[(B^2 - 4B + 3) + 2(1+\alpha_0)(1+\alpha_0 B) \right. \\ & \times \ln \left(\frac{(1+\alpha_0)B}{1+\alpha_0 B} \right) + \alpha_0(B-1)(B^2 - 2B - 1) \left. \right]^2 \end{aligned} \quad (67)$$

[Hsu et al. \(1994\)](#) found that $\alpha_0 = 0.002$ and $\varepsilon = 0.42$ yields the best agreement with data obtained from [Nozad et al. \(1985b\)](#).

[Kaviany \(1991\)](#) presented a model to calculate the contact area between two spheres by using Hertzian elastic deformation principles. The radius of the contact area r_c between two spheres of radius r_p can be calculated by using the Poisson ratio μ_p , the Young modules E_p and a collinear force F acting on the particles. The radius of the contact area is given by:

$$r_c = \left[\left(\frac{3(1-\mu_p^2)}{4E_p} \right) Fr_p \right]^{1/3} \quad (68)$$

[Kaviany \(1991\)](#) then presented the overall thermal conductivity due to the contact area as:

$$\frac{k_e^c}{k_s} = \frac{r_c}{0.531S} \left(\frac{N_A}{N_L} \right) \quad (69)$$

Table 4

Magnitude of structural parameters for different close packing arrangements ([Kaviany, 1991](#)).

Types of packing	Porosity range	N_A	N_L	S	S_F
SC	$\varepsilon : 0.5 - 0.35$	$1/(4r_s^2)$	$1/(2r_s)$	1	1
BCC	$\varepsilon : 0.3 - 0.25$	$3/(16r_s^2)$	$\sqrt{3}/(2r_s)$	0.25	$\sqrt{3}/4$
FCC	$\varepsilon : \leq 0.2$	$1/(4r_s^2)$	$1/(\sqrt{2}r_s)$	1/3	$1/\sqrt{6}$

where the force F is related to the external pressure $p[Pa]$ through $F = p(S_F/N_A)$ with N_A and N_L the number of particles per unit area and unit length respectively. The constants S and S_F are given in [Table 4](#). This model considers a randomly packed bed, to be based on three different ordered structures, depending on porosity. One should however note that certain porosity ranges are not defined in [Table 4](#).

[Robold \(1982\)](#) presented a model where the pebble bed is represented by a system of parallel layers of spherical particles perpendicular to the direction of heat flux. Although only briefly touched on here, the model is explained in full in Section 3.3. The effective thermal conductivity model, neglecting thermal radiation, is given by:

$$k_e^g = k_f \frac{d^e}{d_f^e} \left[1 - \frac{\Delta_0}{1 + \frac{k_s/d_s^e}{F_{E,0}4\sigma T^3 + k_f/d_f^e}} \right] \quad (70)$$

where

$$\Delta_0 = \frac{F_E(1 - B_{r,0}) - B_{r,0}}{F_{E,0}(1 - B_{r,0})} \quad (71)$$

and

$$F_E = \frac{2B_r + \varepsilon_r(1 - B_r)}{(1 - B_r)(2 - \varepsilon_r)} \quad (72)$$

[Robold \(1982\)](#) noted that temperature gradients within the layers of spherical particles have to be addressed and developed a transformed pebble diameter $d^e = d_f^e + d_s^e$, with $d^e = 0.523d_p/(1 - \varepsilon)$, $d_f^e = d^e/(1 + \pi)$ a fluid gap width and $d_s^e = d^e\pi/(1 + \pi)$ a solid thickness parameter. [Robold \(1982\)](#) also developed a model to account for contact area and introduced a contact area parameter s given by:

$$k_e^{g,c} = (1 - s)k_e^g + sk_s \quad (73)$$

[Slavin et al. \(2002\)](#) presented a model to calculate the effective thermal conductivity by including a measurable parameter for particle roughness. With this, the conductivity for an uncompressed bed can be calculated with no adjustable parameters, provided that the conductance of the solid is much larger than the fluid or gas phase. The model was developed for small particles and therefore much attention was given to the Smoluchowski effect. The model treats the particles as perfect spheres, separated at their contact points by a short cylinder of contact area δ and length/height $2h_r$. This cylinder represents the surface roughness of the particle. Due to the nature of the model it cannot be compared with the previously mentioned empirical models. The model is more fundamental based than those previously mentioned and assign each region of heat transfer between two particles with a specific correlation.

[Bahrami et al. \(2004a,b\)](#) and [Bahrami et al. \(2006a,b\)](#) developed a new compact resistance model to predict the effective thermal conductivity of randomly packed beds consisting of rough, mono-sized spheres immersed in a stagnant gas at various gas pressures (from atmospheric to vacuum) and subjected to a range of mechanical loads. [Bahrami et al. \(2006a\)](#) focussed on three heat transfer paths: the interstitial gas within the microgap, microcontacts and the interstitial gas within the macrogap. This model was extended by [Van Antwerpen et al. \(2009\)](#) by incorporating the Smoluchowski

effect into the macrogap, developing a resistance model for the solid region and developing a new thermal radiation correlation between the two adjacent spheres. Due to their fundamental based nature the models described by Slavin et al. (2002), Bahrami et al. (2006a) and Van Antwerpen et al. (2009) are not compared with the other empirical correlations in Section 3.5 due to the lack of experimental parameters.

3.3. Effective thermal conductivity due to thermal radiation

Lee et al. (2001) pointed out that many different methods to simulate the radiative heat transfer in packed sphere systems were developed through the years. These methods can be grouped into three approaches.

The first one is the Radiative Transfer Equation (RTE) approach (Siegel and Howell, 1992; Modest, 1993; Kamiuto et al., 1993). The RTE approach is a radiative energy balance equation for the emitting, absorbing and scattering medium. In order to solve for the intensity distribution in the packing under consideration, a set of optical properties, such as the scattering coefficient, absorption coefficient and phase function, must first be obtained (Lee et al., 2001). Each set of packed sphere systems have their own set of optical properties due to the different microstructures of the individual packings. The optical properties can either be obtained experimentally or numerically. Argento and Bouvard (1996) explained the RTE by considering the so-called two-flux model. However, a comparison between the results of the two-flux model and the Monte Carlo Diffuse model (Fig. 8) shows that the two-flux model gives unrealistic values at low values of the emissivity ε_r .

The second approach is that of the unit cell method (Cheng and Churchill, 1963; Cheng et al., 2002; Kasperek and Vortmeyer, 1976; Vortmeyer, 1978; Robold, 1982; Breitbach and Barthels, 1980). The unit cell approach makes use of repeated units of idealized geometry with the optical properties predetermined. The energy distribution for the system can thus be formulated as a set of simple algebraic equations. The general form for the thermal radiative conductivity for a unit cell in a packed pebble bed is defined as:

$$k_e^r = 4F_E^* \sigma d_p \bar{T}^3 \quad (74)$$

where F_E^* is defined as a radiation exchange factor, σ the Stefan–Boltzmann constant and d_p the particle diameter. Strieder (1997) stated that the thermal radiative conductivity only remains valid as long as we assume that the steady state temperature drop ΔT across the local average bed dimension is much smaller than the average bed temperature \bar{T} , i.e. $\Delta T/\bar{T} \ll 1$. This is due to the fact that most unit cell models make use of an averaging assumption that $(T_1^4 - T_2^4)/(T_1 - T_2) \approx 4\bar{T}^3$ as noted by Van Antwerpen et al. (2009). Early attempts to formulate the radiation exchange factor was made by Kasperek and Vortmeyer (1976) who defined the radiation exchange factor as $F_E = f(\varepsilon, \varepsilon_r)$. However, Singh and Kaviany (1994) demonstrated that the radiant conductivity is strongly influenced by the solid conductivity k_s and particle emissivity ε_r , resulting in the radiation exchange factor to be defined as $F_E^* = f(\Lambda_f, \varepsilon, \varepsilon_r)$ where $\Lambda_f = k_s/4d_p\sigma\bar{T}^3$ is a dimensionless solid conductivity. The single most important limitation of the radiation exchange factor is that the value of F_E or F_E^* cannot be calculated easily, and this led Howell (2000) to state that many researchers have recognized the inaccuracy of this simple approach.

The third approach is that of the Radiative Transfer Coefficient (RTC), developed by Lee et al. (2001). The RTC is a numerical method that can provide average temperature solutions as fine as the size of the spheres. The RTC is a function of the microstructure (coordination number, area of contact and the distance between the centres of the spheres) and radiative properties (reflectivity of sphere surface) of the packed sphere system. In the RTC approach, a set of

algebraic equations is first established to compute the energy in each sphere. With the energy distribution known, the temperature of each sphere can be computed accordingly. The RTC is calculated using a Monte Carlo ray-tracing method. With the known RTC, the set of algebraic equations can be solved using an iterative scheme.

Kunii and Smith (1960) also presented a lumped parameter model consisting of the model described in Eqs. (45)–(48) with radiation added. The model is given by:

$$\frac{k_{eff}}{k_f} = \varepsilon \left[1 + \frac{\beta k_{rv} d_p}{k_f} \right] + \frac{\beta(1 + \varepsilon)}{\left[\frac{1}{1/\psi_t + k_{rs} d_p/k_f} + \frac{\gamma}{\kappa} \right]} \quad (75)$$

where k_{rs} and k_{rv} are the radiation from solid to solid and void to void respectively.

$$k_{rs} = 4\sigma T^3 \left[\frac{\varepsilon_r}{(2 - \varepsilon_r)} \right] \quad (76)$$

and

$$k_{rv} = \left[4\sigma T^3 / 1 + \frac{\varepsilon}{2(1 - \varepsilon)} \frac{(1 - \varepsilon_r)}{\varepsilon_r} \right] \quad (77)$$

As mentioned previously, Kunii and Smith (1960) concluded that $\gamma = 2/3$ and ψ_t as defined in Eq. (46) with T in Kelvin.

A summary of the radiation exchange factors found in the literature is presented in Table 5. Cheng and Churchill (1963) developed a model treating radiative heat transfer as a diffuse process. This model was reworked by Argento and Bouvard (1996) and presented as the dimensionless radiation exchange factor given in Eq. (78). Despite the extensive research done by Cheng and Churchill (1963), Cheng et al. (2002) stated that this model cannot be used in general, because the absorption and scattering coefficients are specific to the packing structure.

Kasperek and Vortmeyer (1976), Vortmeyer (1978), Breitbach (1978) and Robold (1982) all developed and optimized a one-dimensional radiative heat transfer model, where the pebble bed is represented by a system of parallel layers of spherical particles perpendicular to the direction of heat flux as mentioned previously. These layers can also exchange radiation through voids, resulting in an interaction between distant layers. However, each of these models has its own set of radiation transmission numbers B_r that vary with emissivity and no general function is available to calculate B_r for different packing arrangements.

Breitbach (1978) noted the importance of accounting for temperature gradients at high temperatures and low values for the solid conductivity k_s and developed a new set of equations. Robold (1982) on the other hand also noted the importance of temperature gradients within a layer and followed a different methodology. As previously mentioned he introduced a transformed pebble diameter d^e , with a fluid gap width d^f and a solid thickness parameter d^s to address just that. A summation of Eq. (73) and Eq. (85) addresses all the heat transfer phenomena investigated by Robold (1982) with the parameter $K = k_f/d_f^e$ in Eq. (85). If only thermal radiation is investigated with the Robold (1982) correlation, it is done so with Eq. (85) with $K=0$.

Breitbach and Barthels (1980) refined the model presented by Zehner and Schlünder (1972). They noted that an unsatisfactory feature of the Zehner and Schlünder (1972) model is that the unit cell is assumed to be closed and therefore radiation from the voids outside the unit cell is not taken into account. Breitbach and Barthels (1980) changed the correlation by changing the derivation, closing the base areas of the unit cell with black surfaces instead of surfaces having the same emittance as the particles and derived Eq. (84).

Singh and Kaviany (1994) analyzed the effects of solid conductivity on radiative heat transfer in packed beds by developing an empirical correlation with the aid of Monte Carlo simulations. The

Table 5
Summary of radiant exchange factors.

Reference	Radiation exchange factor without consideration of thermal conductivity	Parameters and comments
Cheng and Churchill (1963)	$F_E = \frac{2}{d_p(a + 2b)}$ (78)	Need absorption a and scattering b coefficients for each different packing.
Wakao and Wato (1968)	$F_E = \frac{2}{(2/\varepsilon_r - 0.264)}$ (79)	–
Argo and Smith (1957)	$F_E = \frac{1}{(2/\varepsilon_r - 1)}$ (80)	–
Kasperek and Vortmeyer (1976)	$F_E = \frac{\varepsilon_r + B_r}{1 - B_r}$ (81)	$B_r = 0.149909 - 0.24791\varepsilon_r + 0.290799\varepsilon_r^2 - 0.20081\varepsilon_r^3 + 0.0651042\varepsilon_r^4$ for $\varepsilon = 0.4$ $B_r = 0.179 - 0.24791\varepsilon_r + 0.290799\varepsilon_r^2 - 0.20081\varepsilon_r^3 + 0.0651042\varepsilon_r^4$ for $\varepsilon = 0.48$
Vortmeyer (1978)	$F_E = \frac{2B_r + \varepsilon_r(1 - B_r)}{2(1 - B_r) - \varepsilon_r(1 - B_r)}$ (82)	B_r is calculated the same as for (Kasperek and Vortmeyer, 1976).
Ref	Radiation exchange factor with consideration of thermal conductivity	Comments
Breitbach (1978)	$F_E^* = \left[\frac{\pi}{6} \frac{\psi}{1 - \varepsilon} \times \left(1 - \frac{\tau h(\Lambda_f, \varepsilon_r, \varepsilon)(1 + \psi)}{1 + \psi \tau h(\Lambda_f, \varepsilon_r, \varepsilon)} \right) \right]$ (83)	B_r is calculated as in (Kasperek and Vortmeyer, 1976). $R = (1 - B_r)(1 - \varepsilon_r')$ $\varepsilon_r' = \varepsilon_r / (0.5(1 - \varepsilon_r) + \varepsilon_r)$ $\tau = (1 - B_r - R) / (1 + B_r - R)$ $\psi = (1 + B_r - R) / (1 - B_r + R)$ $h(\Lambda_f, \varepsilon_r, \varepsilon) = \left[1 - 2((B_{r,0} - B_r) / (1 - B_r - R)) \right] \times \varepsilon_r' / ((12/\pi)\Lambda_f(1 - \varepsilon) + \varepsilon_r')$
Breitbach and Barthels (1980)	$F_E^* = \left\{ \left[1 - \sqrt{1 - \varepsilon} \right] \varepsilon + \frac{\sqrt{1 - \varepsilon}}{\frac{2}{\varepsilon_r} - 1} \times \frac{B + 1}{B} \cdot \frac{1}{1 + \frac{1}{\left(\frac{2}{\varepsilon_r} - 1\right)\Lambda_f}} \right\}$ (84)	$B = 1.25 \left((1 - \varepsilon) / \varepsilon \right)^{10/9}$
Robold (1982)	$F_E^* = F_E \left[1 - \chi \frac{\Delta_0}{1 + \frac{k_s}{F_{E,0} 4d_s^2 \sigma T^3 + K}} \right]$ (85)	$B_r = 0.0894306 - 0.14456\varepsilon_r + 0.106337\varepsilon_r^2 + 0.0159144\varepsilon_r^3 - 0.0325521\varepsilon_r^4$ for $\varepsilon = 0.395$ $B_r = 0.0949306 - 0.14456\varepsilon_r + 0.106337\varepsilon_r^2 + 0.0159144\varepsilon_r^3 - 0.0325521\varepsilon_r^4$ for $\varepsilon = 0.43$ $F_E = \frac{2B_r + \varepsilon_r(1 - B_r)}{(1 - B_r)(2 - \varepsilon_r)}$ $\chi = F_{E,0} / F_E$
Singh and Kaviany (1994)	$F_E^* = a_1 \varepsilon_r \tan^{-1} \left(a_2 \frac{(\Lambda_f)^{a_3}}{\varepsilon_r} \right) + a_4$ for $\varepsilon = 0.476$ (86)	$a_1 = 0.5756$ $a_2 = 1.5353$ $a_3 = 0.8011$ $a_4 = 0.1843$

parameters shown in Eq. (86) are for a diffuse surface with a SC packing arrangement.

Cheng et al. (2002) extended their effective thermal conductivity model mentioned previously by the introduction of a radiation correlation. This radiative model uses Voronoi polyhedra to define the packing structure for their numerical calculations.

Lastly, Van Antwerpen et al. (2009) developed a new radiation model by considering the packing arrangement in a more fundamental manner. This has the advantage that the radiative thermal conductivity can be calculated for a randomly packed bed in the bulk region as well as in the near-wall region.

3.4. Effective thermal conductivity in the near-wall region

The previous sections have shown that a large number of correlations have been developed for the stagnant effective thermal conductivity. Although not explicitly noted, it will appear from the open literature found that these correlations have also been used to compute the effective thermal conductivities for stagnant flow in cases where there are large variations in the porosity, especially in the near-wall region. Van der Merwe et al. (2006), for example, demonstrated the limitations of the correlation proposed by IAEA-

TECDOC-1163 (2000) for the simulation of the heat transfer at the interface between the pebble bed and the reflector.

Thurgood et al. (2004) investigated the applicability of some effective thermal conductivity correlations in the near-wall region by considering the correlations proposed by Kunii and Smith (1960) and Schlünder and co-workers (Zehner and Schlünder, 1970; Bauer and Schlünder, 1978). The results demonstrated the inability of these correlations to simulate the heat transfer in the near-wall region at high temperatures. This may be attributed to the effect of the reactor wall in the near-wall region where it forces the pebbles in contact with the wall into a nearly ordered arrangement. Each pebble touches the wall only at one point. This solitary contact with the wall greatly reduces heat flow from the pebble to the wall when radiation is neglected. This is usually because heat flow has to travel through the low conductivity gas before reaching the reactor wall (Thurgood et al., 2004). The Smoluchowski effect contributes significantly in this respect.

Thurgood et al. (2004) defined limiting boundaries for the effective thermal conductivity in the near-wall region. Firstly, when (neglecting any contribution by radiation) the void fraction ε approaches unity (pure fluid) the effective thermal conductivity becomes $k_{eff}/k_f = 1$ at $\varepsilon = 1$. Secondly, if the solid and fluid/gas con-

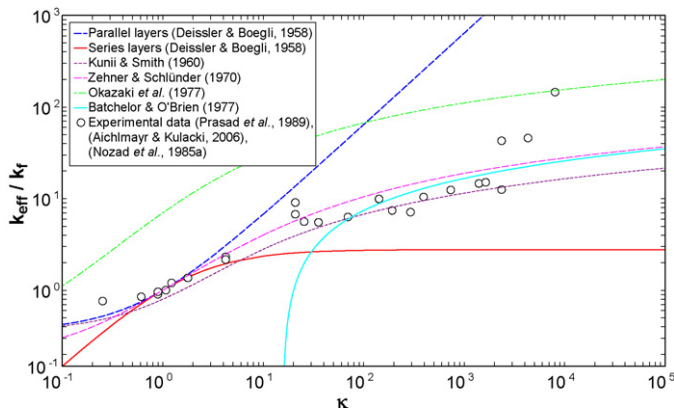


Fig. 5. Effective thermal conductivity models at $\varepsilon = 0.36$ (neglecting contact area) versus experimental results.

ductivity have the same values the effective thermal conductivity must be the same $k_s = k_f = k_{eff}$. Thurgood et al. (2004) also stated that the effective thermal conductivity is expected to decrease with an increase in porosity. This is a simple consequence of reducing the number of high conductivity particles and replacing them with low conductivity gas. This was also noted by Du Toit et al. (2009) who observed a decrease in the coordination number as the wall is approached.

Yagi and Kunii (1961) proposed a modification to the Kunii and Smith (1960) model for the near-wall region. The model simplified the near-wall region by confining the porosity to $\varepsilon_{wall} = 0.7$. However, in the analysis of Thurgood et al. (2004) the porosity was allowed to vary. The model resulted in a decrease in the effective thermal conductivity with thermal radiation included. Another observation was that the effective thermal conductivity ratio k_{eff}/k_f was higher than 1 when $\varepsilon = 1$.

Tsotsas (2002) also proposed an additional term to the ZBS correlation. However, Thurgood et al. (2004), as well as Visser et al. (2005) noted that the model proposed by Tsotsas (2002) is not continuous with the parent correlation ZBS when simulating the near-wall region.

Therefore, due to the inability of these models to simulate the effective thermal conductivity in the near-wall region it was decided not to include them in this study.

For that reason Van Antwerpen et al. (2009) developed a correlation which can simulate the effective thermal conductivity in the bulk region, as well as the near-wall region.

3.5. Comparison between effective thermal conductivity correlations

The generally accepted method to compare effective thermal conductivity data is to normalize the solid and effective thermal conductivities with respect to the fluid thermal conductivities, subsequently generating a dimensionless chart. Interpreting the minimum and maximum effective thermal conductivity of Deissler and Boegli (1958) for a two-phase system reveals the results displayed in Fig. 5.

Experimental measurements for any porous media arrangement saturated with a stagnant fluid should fall inside the minimum and maximum bounds proposed by Deissler and Boegli (1958) as long as no natural convection occurs. Aichlmayr (1999) noted that even though the literature abounds with measurements of effective thermal conductivity, there is a lack of uncertainty estimates for the experimental results. Hence, the quality of the measurements presented in the literature is not available.

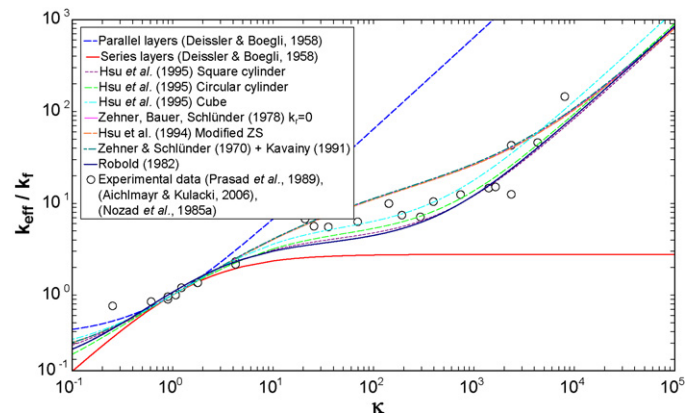


Fig. 6. Effective thermal conductivity models at $\varepsilon = 0.36$ (contact area included) versus experimental results.

Nonetheless, the experimental measurements presented by Prasad et al. (1989), Aichlmayr and Kulacki (2006) and Nozad et al. (1985a) were used to evaluate the effective thermal conductivity models neglecting the contribution due to thermal radiation.

Nield (1991), however, questioned the accuracy of the results published by Prasad et al. (1989) for $\kappa < 1$, because he noted that some of the effective thermal conductivity ratios were not within the bounds of the maximum and minimum values given by the series and parallel models as shown in Fig. 5. However, for the purpose of this study we will leave the data as published. A full in-depth analysis of the experimental measurements for saturated porous media is given in Aichlmayr and Kulacki (2006).

A study of Fig. 5 reveals the failure of the Kunii and Smith (1960), Zehner and Schlünder (1970) and Batchelor and O'Brien (1977) models when $\kappa > 10^3$. The inability of these models to capture the change in trend of the effective thermal conductivity data can be attributed to the fact that they neglect the details of the contact area in their models. Therefore, the models presented in Section 3.2 that account for the contact area results in Fig. 6.

The models proposed by Hsu et al. (1995) and Zehner, Schlünder and co-workers agree well with the experimental data. It should be noted that each of these models have a specific contact area variable that must be determined to obtain agreement with the experimental data. Each parameter was evaluated to obtain the best fit with the experimental data. Important to note is that $\bar{\varepsilon}_r = 0.88$ was assumed for the Robold (1982) model in Eq. (70). A summary of these parameters are displayed in Table 6.

Another important aspect to be addressed is the range of porosities over which the various effective thermal conductivity models are applicable. This tests one of the limiting factors mentioned by Thurgood et al. (2004) where the effective thermal conductivity must approach $k_{eff}/k_f = 1$ at $\varepsilon = 1$. In Fig. 7 the porosity was varied between $0.2595 \leq \varepsilon \leq 1$.

Table 6
Contact area constants for models evaluated in Fig. 6.

Author	Contact area parameter
Hsu et al. (1995) Square cylinder	$\gamma_c = 0.01$
Hsu et al. (1995) Circular cylinder	$\gamma_c = 0.01$
Hsu et al. (1995) Cube	$\gamma_c = 0.13$
Bauer and Schlünder (1978)	$\varphi = 0.01$
Hsu et al. (1994)	$\alpha_0 = 0.002$
Zehner and Schlünder (1970) + Kaviany (1991)	$p = 2 \times 10^3$ [Pa]
Robold (1982)	$s = 0.0085$

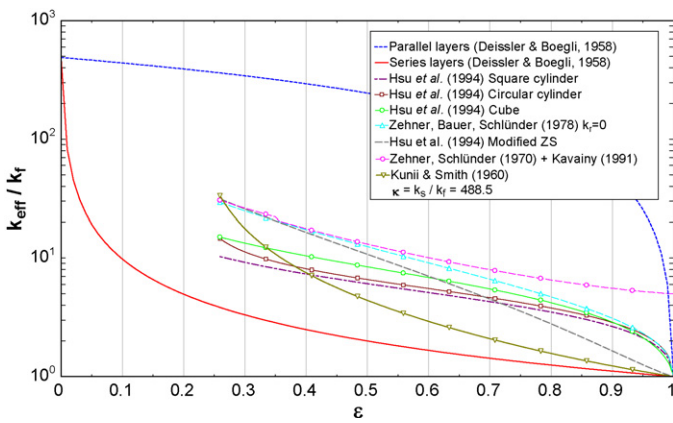


Fig. 7. Effective thermal conductivity models (contact area included, radiation neglected) versus porosity variation.

It can be seen that the summation of the Zehner and Schlünder (1970), Eq. (49) and Kaviany (1991), Eq. (69) models does not approach unity when $\varepsilon = 1$. The reason is that in the Kaviany (1991) model certain parameters were assigned values based on three ordered packings for a specific limited range of porosities. It is therefore a significantly simplified approximation of a complex porous structure and should be treated as such.

Kasperek and Vortmeyer (1976) studied the radiation heat transfer in a packed bed in the case where contact area was eliminated. Radiation heat transfer measurements were taken through a number of sphere layers where conduction and convection were eliminated by introducing a small gap between sphere layers and testing under vacuum conditions. Ultimately, they obtained radiation exchange factor measurements, F_E , for different emissivities and porosities. Table 7 presents the numerical and experimental data developed and obtained by Singh and Kaviany (1994) and Kasperek and Vortmeyer (1976) for the radiation exchange factor F_E at various emissivities.

Comparing the F_E and F_E^* models listed in Table 5 with the experimental and numerical data yields the results displayed in Fig. 8.

Fig. 8 clearly demonstrates a difference between the F_E and F_E^* models and the numerical and experimental data. It can, thus, be concluded that this aspect needs to be investigated in greater depth.

Finally, the IAEA-TECDOC-1163 (2000) proposed that the effective thermal conductivity can be calculated as the summation of Eqs. (49), (69) and (84), denoted as Total k_{eff} in this study.

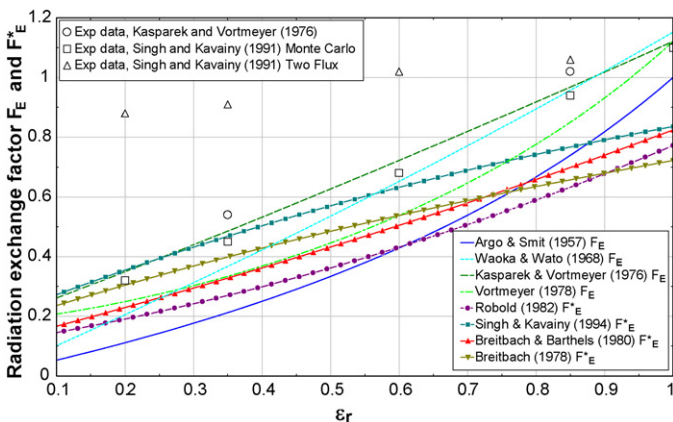


Fig. 8. Comparison of F_E and F_E^* models with emissivity with $T = 1067^\circ\text{C}$, $\varepsilon = 0.43$ and $k_s = 30 \text{ W m}^{-1} \text{ K}^{-1}$.

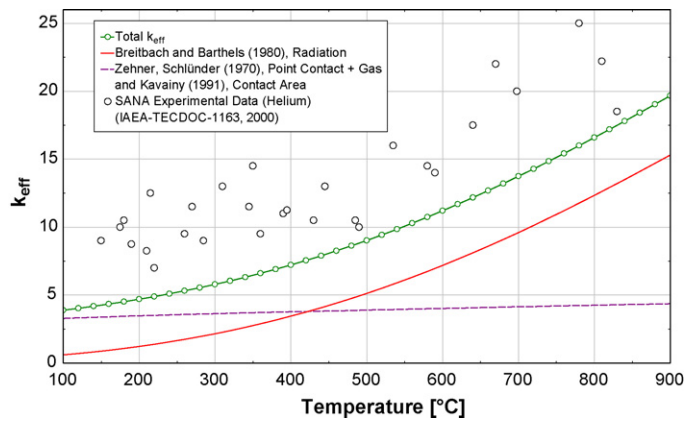


Fig. 9. Comparison with SANA helium experimental data $d_p = 0.06 \text{ m}$, $\varepsilon = 0.385$, $\varepsilon_r = 0.8$.

Comparing the three different components with the effective thermal conductivity measurements obtained from the SANA helium experiments (IAEA-TECDOC-1163, 2000), led to the results displayed in Fig. 9.

The comparison of the predictions of the effective thermal conductivity correlations and measured data obtained in the SANA experiment shows that the predicted effective thermal conductivity is lower than the values obtained from the measurements. The reason is that in the SANA experiment the heat is not only transported by thermal radiation and conduction alone, but also by natural convection of the gas in the pebble bed (IAEA-TECDOC-1163, 2000). In the correlation used for the analysis in Fig. 9, the effect of the natural convection in the packed bed is not incorporated.

A comparison of the predictions by other correlations with the SANA helium experimental results yields the results displayed in Fig. 10.

The correlation proposed by Robold (1982) yields values that is much lower than the data presented by the IAEA-TECDOC-1163 (2000) and the values predicted by the correlations proposed by Bauer and Schlünder (1978) and Kunii and Smith (1960). However, Hoffmann (2003) investigated the effective conductivity through a SC using Computational Fluid Dynamics (CFD) and observed that the Robold (1982) correlation yields better values for $T \geq 2000^\circ\text{C}$. However, due to the extreme simplification of the complex packing structure by Hoffmann (2003), this statement should be re-evaluated when considering a randomly packed bed.

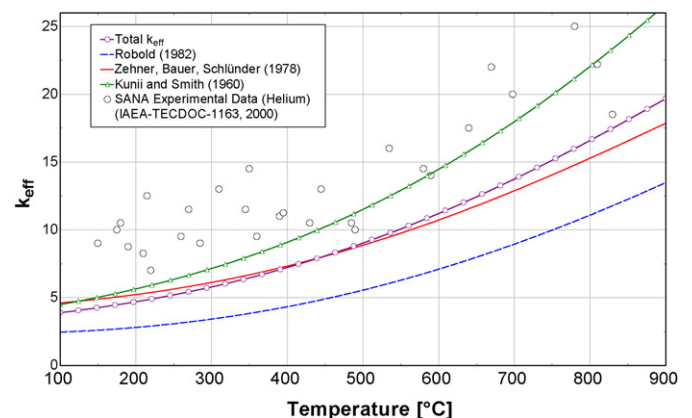


Fig. 10. Comparison with SANA helium experimental data, $d_p = 0.06 \text{ m}$, $\varepsilon = 0.385$ and $\varepsilon_r = 0.8$.

Table 7Numerical and experimental data for the radiation exchange factor F_E .

Reference	Method	Emissivity				
		0.20	0.35	0.60	0.85	1.0
		Radiation exchange values F_E				
Singh and Kaviany (1994)	Monte Carlo (Diffuse)	0.32	0.45	0.68	0.94	1.10
Singh and Kaviany (1994)	Two-Flux (Diffuse)	0.88	0.91	1.02	1.06	1.11
Kasperek and Vortmeyer (1976)	Experimental ($\varepsilon = 0.4$)	–	0.54	–	1.02	–

4. Conclusion

This paper presented an in-depth analysis of the determination of the packing structure and effective thermal conductivity of mono-sized spherical packed beds. However, it is noted that there is a tendency to move away from the use of purely empirical correlations to the analysis of numerically simulated packed beds. This enables researchers to develop models that distinguish more clearly between the various contributing phenomena as was done by Bahrami et al. (2006a) and Van Antwerpen et al. (2009).

When the heat transfer in a packed bed is considered the effect of the packing structure cannot be characterized by the porosity alone. The variation of coordination number and the contact angles between adjacent particles must also be considered. It was shown that in the near-wall region in particular that the coordination number is not predicted correctly in most cases.

It has been found that reasonable accuracy can be obtained with the unit cell approach of Schlünder and co-workers in the bulk region of a randomly packed bed. This is also the method commonly used to calculate the effective thermal conductivity in the core of high temperature gas-cooled nuclear reactors. However, caution should be taken when using the unit cell model in the near-wall region.

Acknowledgements

The authors wish to thank the North-West University, PBMR (Pty) Ltd. and M-Tech Industrial (Pty) Ltd. In South Africa whose financial support made this work possible.

References

- Aichlmayr, H.T., Kulacki, F.A., 2006. Effective conductivity of saturated porous media. *Advances in Heat Transfer* 39, 377–460.
- Aichlmayr, H.T., 1999. The effective thermal conductivity of saturated porous media, University of Minnesota, Masters Thesis.
- Anon, 1999. PFC3D (Particle Flow Code in 3D): Theory and Background Manual 2. Itasca Consulting Group Inc., Minneapolis.
- Argento, C., Bouvard, D., 1996. A ray tracing method for evaluating the radiative heat transfer in porous media. *International Journal of Heat and Mass Transfer* 39, 3175–3180.
- Argo, W.B., Smith, J., 1957. Heat transfer in packed beds. *Chemical Engineering Progress* 49, 443–451.
- Bahrami, M., Culham, J.R., Yovanovich, M.M., 2006b. Review of thermal joint resistance models for nonconforming rough surfaces. *Applied Mechanics Reviews* 59, 1–12.
- Bahrami, M., Yovanovich, M.M., Culham, J.R., 2004a. Thermal joint resistance of conforming rough surfaces with gas-filled gaps. *Journal of Thermophysics and Heat Transfer* 18, 318–325.
- Bahrami, M., Yovanovich, M.M., Culham, J.R., 2004b. Thermal joint resistance of non-conforming rough surfaces with gas-filled gaps. *Journal of Thermophysics and Heat Transfer* 18, 326–332.
- Bahrami, M., Yovanovich, M.M., Culham, J.R., 2006a. Effective thermal conductivity of rough spherical packed beds. *International Journal of Heat and Mass Transfer* 49, 3691–3701.
- Batchelor, G.K., O'Brien, R.W., 1977. Thermal or electrical conduction through a granular material. *Proceedings of the Royal Society of London, Series A* 355, 313–333.
- Bauer, R., Schlünder, E.U., 1978. Part I: Effective radial thermal conductivity of packings in gas flow. Part II: Thermal conductivity of the packing fraction without gas flow. *International Chemical Engineering* 18, 189–204.
- Bauer, R., 1990. Stagnant packed beds. In: Hewitt, G.F. (Ed.), *Hemisphere Handbook of Heat Exchanger Design*. Hemisphere Publishing Corporation, pp. 2.8.1–2.8.4–14.
- Benenati, R.F., Brosilow, C.R., 1962. Void fraction distribution in beds of spheres. *AIChE Journal* 8, 359–361.
- Breitbach, G., Barthels, H., 1980. The radiant heat transfer in the high temperature reactor core after failure of the afterheat removal systems. *Nuclear Technology* 49, 392–399.
- Breitbach, G., 1978. Wärmetransportvorgänge unter besonderer Berücksichtigung der Strahlung. Jül-1564, Nuclear Research Center Jülich.
- Cheng, G.J., Yu, A.B., Zulli, P., 1999. Evaluation of effective thermal conductivity from the structure of a packed bed. *Chemical Engineering Science* 54, 4199–4209.
- Cheng, G.J., Yu, A.B., Zulli, P., Xu, D.L., 2002. Radiation heat transfer in random packing of mono-sized spheres. In: *Proceedings of the 4th World Congress on Particle Technology*, Paper No. 313, Sydney, Australia.
- Cheng, J.C., Churchill, S.W., 1963. Radiant transfer in packed beds. *AIChE Journal* 9, 35–41.
- Cheng, P., Hsu, C.T., 1986. Fully-developed, forced convection flow through an annular packed-sphere bed with wall effects. *International Journal of Heat and Mass Transfer* 29, 1843–1853.
- Cho, H.H., Eckert, E.R.G., 1994. Transition from transpiration to film cooling. *International Journal of Heat and Mass Transfer* 37, 3–8.
- Cohen, Y., Metzner, A.B., 1981. Wall effects in laminar flow of fluids through packed beds. *AIChE Journal* 8, 359–361.
- Currie, J.A., 1960. Gaseous diffusion in porous media, Part 1. A non-steady state method; Part 2. Dry granular materials. *British Journal of Applied Physics* 11, 314–317, 318–324.
- De Klerk, A., 2003. Voidage variation in packed beds at small column to particle diameter ratio. *AIChE Journal* 49, 2022–2029.
- Deissler, R.G., Boegli, J.S., 1958. An investigation of effective thermal conductivities of powders in various gases. *ASME Transactions* 80, 1417–1425.
- Du Toit, C.G., 2008. Radial variation in porosity in annular packed beds. *Nuclear Engineering and Design* 238, 3073–3079.
- Du Toit, C.G., Van Antwerpen, W., Rousseau, P.G., 2009. Analysis of the porous structure of an annular pebble bed reactor. In: *ICAPP 2009 Conference*, Paper ID 9123.
- Fogler, H.S., 1999. *Elements of Chemical Reaction Engineering*, 3rd ed. Prentice-Hall.
- Georgalli, G.A., Reuter, M.A., 2006. Modelling the co-ordination number of a packed bed of spheres with distributed sizes using a CT scanner. *Minerals Engineering* 19, 246–255.
- Giese, M., Rottschäfer, K., Vortmeyer, D., 1998. Measured and modeled superficial flow profiles in packed beds with liquid flow. *AIChE Journal* 44, 484–490.
- Goodling, J.S., Khader, M.S., 1985. Co-ordination number distribution of spherical particles in a packed cylindrical bed. *Powder Technology* 44, 53–55.
- Goodling, J.S., 1985. Co-ordination number distribution of spherical particles in a packed cylindrical bed. *Powder Technology* 44, 53–55.
- Goodling, J.S., Vachon, R.I., Stelpflug, W.S., Ying, S.J., 1983. Radial porosity distribution in cylindrical beds packed with spheres. *Powder Technology* 35, 23–29.
- Gotoh, K., 1978. *Journal of the Society of Powder Technology* 15, 220.
- Haughey, D.P., Beveridge, G.S.G., 1969. Structural properties of packed beds—a review. *Canadian Journal of Chemical Engineering* 47, 130–140.
- Hindrichsen, H., Wolf, D.E., 2006. *The Physics of Granular Media*. Published by Wiley, pp. 55.
- Hoffmann, J.E., 2003. Effective conductivity of a composite pebble bed. *PBM Document*, pp. 260-019229-4003.
- Howell, J.R., 2000. *Handbook of Porous Media*. Marcel Dekker, Chapter 15.
- Hsu, C.T., Cheng, P., Wong, K.W., 1994. Modified Zehner–Schlünder models for stagnant thermal conductivity of porous media. *International Journal of Heat and Mass Transfer* 37, 2751–2759.
- Hsu, C.T., Cheng, P., Wong, K.W., 1995. A lumped parameter model for stagnant thermal conductivity of spatially periodic porous media. *ASME Journal of Heat Transfer* 117, 264–269.
- Hunt, M.L., Tien, C.L., 1990. Non-Darcian flow, heat and mass transfer in catalytic packed-bed reactors. *Chemical Engineering Science* 45, 55–63.
- IAEA-TECDOC-1163, 2000. Heat transport and afterheat removal for gas cooled reactors under accident conditions. IAEA, Vienna.
- Kamiuto, K., Iwamoto, M., Nagumo, Y., 1993. Combined conduction and correlated-radiation heat transfer in packed beds. *Journal of Thermophysics and Heat Transfer* 7, 496–501.
- Kamiuto, K., Nagumo, Y., Iwamoto, M., 1989. Mean effective thermal conductivities of packed-sphere systems. *Applied Energy* 34, 213.
- Kasperek, G., Vortmeyer, D., 1976. Wärmestrahlung in Schüttungen aus Kugeln mit Vernachlässigbaren Wärmeleitwiderstand. *Wärme- und Stoffübertragung* 9, 117–128.

- Kaviany, M., 1991. Principles of Heat Transfer in Porous Media. Springer-Verlag, pp. 126–127.
- Kennard, E.H., 1938. Kinetic Theory of Gases. McGraw-Hill, New York, London, pp. 305.
- Koster, A., Matzner, H.D., Nichols, D.R., 2003. PBMR design for the future. Nuclear Engineering and Design 222, 231–245.
- Küfner, R., Hofmann, H., 1990. Implementation of radial porosity and velocity distribution in a reactor model for heterogeneous catalytic gas phase reactions (Torus-model). Chemical Engineering Science 45, 2141–2146.
- Kugeler, K., Schulten, R., 1989. Hochtemperaturreaktortechnik. Springer-Verlag, Heidelberg.
- Kunii, D., Smith, J.M., 1960. Heat transfer characteristics of porous rocks. AIChE Journal 6, 71–78.
- Lee, S.H.-K., Ip, S.C.-H., Wu, A.K.C., 2001. Sphere-to-sphere radiative transfer coefficient for packed sphere system. ASME International Mechanical Engineering Congress and Exposition, 105–110.
- Martin, H., 1978. Low peclet number particle-to-fluid heat and mass transfer in packed beds. Chemical Engineering Science 33, 913–919.
- Meissner, H.P., Micheals, A.S., Kaiser, R., 1964. Crushing strength of zinc oxide agglomerates. Process Design and Development 3, 202–205.
- Modest, M.F., 1993. Radiative Heat Transfer. McGraw-Hill.
- Mueller, G.E., 1991. Prediction of radial distributions in randomly packed fixed beds of uniformly sized spheres in cylindrical containers. Chemical Engineering Science 46, 706–708.
- Mueller, G.E., 1992. Radial void fraction distribution in randomly packed fixed beds of uniformly sized spheres in cylindrical containers. Powder Technology 72, 269–275.
- Mueller, G.E., 1999. Radial void correlation for annular packed beds. AIChE Journal 45, 2458–2460.
- Mueller, G.E., 2002. Narrow annular packed-bed radial void fraction correlation. AIChE Journal 48, 644–647.
- Mueller, G.E., 2005. Numerically packing spheres in cylinders. Powder Technology 159, 105–110.
- Nakagaki, M., Sunada, H., 1968. Theoretical studies on structures of the sedimentation bed of spherical particles. Yakugaku Zasshi 88, 651–655.
- Nield, D.A., 1991. Estimation of the stagnant thermal conductivity of saturated porous media. International Journal of Heat and Mass Transfer 34, 1575–1576.
- Nozad, S., Carbonell, R.G., Whitaker, S., 1985a. Heat conduction in multiphase systems. I. Theory and experiments for two-phase systems. Chemical Engineering Science 40, 843–855.
- Nozad, S., Carbonell, R.G., Whitaker, S., 1985b. Heat conduction in multiphase systems. II. Experimental method and results for three-phase systems. Chemical Engineering Science 40, 857–863.
- Nuclear Safety Standards Commission (KTA), 1981. KTA 3102.3 Reactor Core Design of High-Temperature Gas-Cooled Reactors Part 3: Loss of Pressure through Friction in Pebble Bed Cores, KTA Safety Standard Issue 03/81, Germany.
- Okazaki, M., Yamasaki, T., Gotoh, S., Toei, R., 1977. Effective thermal conductivities of wet granular materials. AIChE Symposium Series 163, 164–176.
- Prasad, V., Kladias, N., Bandyopadhyaya, A., Tian, Q., 1989. Evaluation of correlations for stagnant thermal conductivity of liquid-saturated porous beds of spheres. International Journal of Heat and Mass Transfer 32, 1793–1796.
- Ridgway, K., Tarbuck, K.J., 1966. Radial voidage variation in randomly-packed beds of spheres of different sizes. Journal of Pharmacy and Pharmacology 18, 168S–175S.
- Ridgway, K., Tarbuck, K.J., 1968. Voidage fluctuations in randomly-packed beds of spheres adjacent to a containing wall. Chemical Engineering Science 23, 1147–1155.
- Roble, L.H.S., Baird, R.M., Tierney, J.W., 1958. Radial porosity variations in packed beds. AIChE Journal 4, 460–464.
- Robold, K., 1982. Wärmetransport im Inneren und in der Randzone von Kugelschüttungen. Dissertation Jül-1796, Nuclear Research Center Jülich.
- Rumpf, H., 1958. Grundlagen und Methoden des Granulierens. Chemie Ingenieur Technik 30, 144–158.
- Scott, G.D., 1962. Radial distribution of the random close packing of equal spheres. Nature 194, 956–957.
- Sederman, A.J., Alexander, P., Gladden, L.F., 2001. Structure of packed beds probed by magnetic resonance imaging. Powder Technology 117, 255–269.
- Siegel, R., Howell, J.R., 1992. Thermal Radiation Heat Transfer. Hemisphere Publishing Corporation, London.
- Singh, B.P., Kaviany, M., 1994. Effect of solid conductivity on radiative heat transfer in packed beds. International Journal of Heat and Mass Transfer 37, 2579–2583.
- Slavin, A.J., Arcas, V., Greenhalgh, C.A., Irvine, E.R., Marchalli, D.B., 2002. Theoretical model for the thermal conductivity of a packed bed of solid spheroids in the presence of a static gas, with no adjustable parameters except at low pressure and temperature. International Journal of Heat and Mass Transfer 45, 4151–4161.
- Smith, W.O., Foote, P.D., Busang, P.F., 1929. Packing of homogeneous spheres. Physical Review 34, 1271–1274.
- Sodré, J.R., Parise, J.A.R., 1998. Fluid flow pressure drop through an annular bed of spheres with wall effects. Experimental Thermal and Fluid Science 17, 265–275.
- Song, S., Yovanovich, M.M., 1987. Correlation of thermal accommodation coefficient for engineering surfaces. In: National Heat Transfer Conference, Pittsburgh.
- Springer, G.S., 1971. Heat transfer in rarefied gasses. Advances in Heat Transfer 7, 4151–4161.
- Staněk, V., Eckert, V., 1979. A study of the area porosity profiles in a bed of equal-diameter spheres confined by a plane. Chemical Engineering Science 34, 933–940.
- Strieder, W., 1997. Radiation heat transport in disordered media. Advances in Water Resources 20, 171–187.
- Sui, W.W.M., Lee, S.H.K., 2000. Effective conductivity computation of a packed bed using constriction resistance and contact angle effects. International Journal of Heat and Mass Transfer 43, 3917–3924.
- Suzuki, M., Makino, K., Yamada, M., Inoya, K., 1981. A study on the coordination number in a system of randomly packed, uniform-sized spherical particles. International Chemical Engineering 21, 482–488.
- Thadani, M.C., Peebles, F.N., 1966. Variation of local void fraction in randomly packed beds of equal spheres. Industrial and Engineering Chemistry Process Design and Development 5, 265–268.
- Theuerkauf, J., Witt, P., Schwesig, D., 2006. Analysis of particle porosity distribution in fixed beds using the discrete element method. Powder Technology 165, 92–99.
- Thurgood, C.P., Amphlett, J.C., Mann, R.F., Peppley, B.A., 2004. Radiative heat transfer in packed-beds: the near-wall region. In: AIChE Spring National Meeting, New Orleans April 25–29, Paper No. T2007-16e.
- Tien, C.L., Cunningham, G.R., 1973. Cryogenic insulation heat transfer. Advances in Heat Transfer 9, 349–417.
- Tsotsas, E., Martin, H., 1987. Thermal conductivity of packed beds: a review. Chemical Engineering Processes 22, 19–37.
- Tsotsas, E., 2002. In: Hewitt, G.F. (Ed.), Heat Exchanger Design Handbook. Begell House Publishing, Section 2.8.2.
- Van Antwerpen, W., Rousseau, P.G., Du Toit, C.G., 2009. Accounting for porous structure in effective thermal conductivity calculations in a pebble bed reactor. In: ICAPP 2009 Conference, Paper ID 9124.
- Van der Merwe, J., Van Antwerpen, H.J., Mulder, E.J., 2006. Heat transfer correlation limitations at the pebble bed-reflector interface. In: HTR2006 Conference, Paper number C00000130.
- Visser, C.J., Malan, A.G., Meyer, J.P., 2005. An artificial compressibility algorithm for modeling natural convection in saturated packed pebble beds: a heterogeneous approach. International Journal of Numerical Methods in Engineering 5, 1–6.
- Vortmeyer, D., Schuster, J., 1983. Evaluation of steady flow profiles in rectangular and circular packed beds by a variational method. Chemical Engineering Science 38, 1691–1699.
- Vortmeyer, D., 1978. Radiation in Packed Solids. In: Proceedings, 6th International Heat Transfer Conference (Toronto), vol. 6, pp. 525–539.
- Wakao, N., Wato, K., 1968. Effective thermal conductivity of packed beds. Journal of Chemical Engineering 2, 24–33.
- Whitaker, S., 1980. Heat and mass transfer in granular porous media. Advances in Drying 1, 23–61.
- White, S.M., Tien, C.L., 1987. Analysis of flow channeling near the wall in packed beds. Wärme- und Stoffübertragung 21, 291–296.
- Yagi, S., Kunii, D., 1961. International developments in heat transfer. International Heat Transfer Conference, 760–769.
- Yang, R.Y., Zou, R.P., Yu, A.B., 2000. Computer simulation of the packing of fine particles. Physical Review E 62, 3900–3908.
- Zehner, P., Schlünder, E.U., 1970. Wärmeleitfähigkeit von Schüttungen bei mäßigen Temperaturen. Chemie Ingenieur Technik 42, 933–941.
- Zehner, P., Schlünder, E.U., 1972. Einfluss der Wärmestrahlung und des Druckes auf den Wärmetransport in nicht durchströmten Schüttungen. Chemie Ingenieur Technik 44, 1303–1308.
- Zhang, Z.P., Liu, L.F., Yuan, A.B., Yu, A.B., 2001. A simulation study of the effects of dynamic variables on the packing of spheres. Powder Technology 116, 23–32.
- Zhou, J., Yu, A.B., Zhang, Y., 2007. A boundary element method for evaluation of the effective thermal conductivity of packed beds. Journal of Heat Transfer 129, 363–371.
- Zou, R.P., Yu, A.B., 1995. The packing of spheres in a cylindrical container: the thickness effect. Chemical Engineering Science 50, 1504–1507.